

# Performance of WRF-Chem over Indian region: Comparison with measurements

GAURAV GOVARDHAN<sup>1</sup>, RAVI S NANJUNDIAH<sup>1,2,\*</sup>, S K SATHEESH<sup>1,2</sup>,  
K KRISHNAMOORTHY<sup>3</sup> and V R KOTAMARTHI<sup>4</sup>

<sup>1</sup>*Centre for Atmospheric and Oceanic Sciences, Indian Institute of Science, Bengaluru 560 012, India.*

<sup>2</sup>*Divecha Centre for Climate Change, Indian Institute of Science, Bengaluru 560 012, India.*

<sup>3</sup>*Indian Space Research Organization Headquarters, Bengaluru 560 231, India.*

<sup>4</sup>*Climate Research Section, Environmental Science Division, Argonne National Laboratory, Argonne, IL, United States.*

\*Corresponding author. e-mail: ravi@caos.iisc.ernet.in

The aerosol mass concentrations over several Indian regions have been simulated using the online chemistry transport model, WRF-Chem, for two distinct seasons of 2011, representing the pre-monsoon (May) and post-monsoon (October) periods during the Indo-US joint experiment ‘Ganges Valley Aerosol Experiment (GVAX)’. The simulated values were compared with concurrent measurements. It is found that the model systematically underestimates near-surface BC mass concentrations as well as columnar Aerosol Optical Depths (AODs) from the measurements. Examining this in the light of the model-simulated meteorological parameters, we notice the model overestimates both planetary boundary layer height (PBLH) and surface wind speeds, leading to deeper mixing and dispersion and hence lower surface concentrations of aerosols. Shortcoming in simulating rainfall pattern also has an impact through the scavenging effect. It also appears that the columnar AODs are influenced by the unrealistic emission scenarios in the model. Comparison with vertical profiles of BC obtained from aircraft-based measurements also shows a systematic underestimation by the model at all levels. It is seen that concentration of other aerosols, viz., dust and sea-salt are closely linked with meteorological conditions prevailing over the region. Dust is higher during pre-monsoon periods due to the prevalence of north-westerly winds that advect dust from deserts of west Asia into the Indo-Gangetic plain. Winds and rainfall influence sea-salt concentrations. Thus, the unrealistic simulation of wind and rainfall leads to model simulated dust and sea-salt also to deviate from the real values; which together with BC also causes underperformance of the model with regard to columnar AOD. It appears that for better simulations of aerosols over Indian region, the model needs an improvement in the simulation of the meteorology.

---

## 1. Introduction

Aerosols affect the Earth’s radiation budget by scattering and absorbing the incoming solar and outgoing terrestrial radiations (the direct effect) (Haywood and Ramaswamy 1998; Haywood and Boucher 2000; Kaufman *et al.* 2002; Takemura *et al.*

2005; Yu *et al.* 2006; Myhre 2009) and indirectly by modifying the clouds (Twomey 1977; Lohmann and Lesins 2002; Lohmann and Feichter 2005; Kiran *et al.* 2009). Aerosols such as black carbon (BC) and dust, absorb solar and terrestrial radiation and warm the atmosphere, while hygroscopic aerosols acting as cloud condensation nuclei lead

**Keywords.** Aerosols; black carbon; modelling.

to increase in cloud droplet (for fixed cloud liquid water) number density, leading to smaller cloud droplets, and consequently higher cloud albedo (the first indirect effect) (Twomey 1977). Though the global aerosol abundance (by mass) is dominated by natural aerosols such as sea-salt and dust, the anthropogenic species such as sulphates, nitrates, soot, and organics dominate in areas of high population density, industrialization and urbanization, and areas involving biomass burning (Satheesh and Moorthy 2005; Nair *et al.* 2007). Due to its diverse and contrasting geographical features and the synoptic meteorological conditions that control the Asian monsoon, south Asia is quite vulnerable to the adverse impact of climate change. Composite aerosol concentrations (both natural and anthropogenic) over south Asia have shown an increasing trend; the causes of which could be local and remote sources (Moorthy *et al.* 2013b). Effects of aerosols on the Asian Monsoon system has been a topic of significant interest in the recent years (Ramanathan *et al.* 2001, 2005; Chung *et al.* 2002; Menon *et al.* 2002; Chakraborty *et al.* 2004; Lau *et al.* 2006; Meehl *et al.* 2008; Krishnamurti *et al.* 2009; Gautam *et al.* 2009; Wang *et al.* 2009; Bollasina *et al.* 2011; Ganguly *et al.* 2012; Sajani *et al.* 2012). Simulations carried out by Chakraborty *et al.* (2004) and Lau *et al.* (2006) have indicated an overall increase in monsoonal rainfall (on intra-seasonal to inter-annual time scales) over Indian region due to the atmospheric warming by absorbing aerosols. While studies like Ramanathan *et al.* (2005), Bollasina *et al.* (2011) have suggested a reduction in monsoonal rainfall (on decadal time scales) due to the overall increased abundance of aerosols over the south Asian region. The above model simulations involve use of some kind of chemistry-transport model (offline/online). As such, accurate simulations of aerosols over Indian and Asian regions assume importance for better climate impact assessment, understanding implications on monsoon, and also for planning mitigation strategies. Earlier works on simulations of aerosols over Indian region have brought out certain limitations in some of the regional and global models such as GOCART or RegCM (Nair *et al.* 2012; Moorthy *et al.* 2013a). Carrying out a performance evaluation of Regional Climate Model (RegCM4) over south Asia, Nair *et al.* (2012) have shown that while there has been a good agreement in simulating the columnar AODs over the desert region, however, the model underestimated the AODs at the stations where there was a significant anthropogenic influence. Additionally, they reported an underestimation of near-surface BC by RegCM4 model in comparison with the surface observations and the underestimation was higher during winter and

night-time (periods of shallower and more stable atmospheric boundary layer conditions). The authors attributed the model BC and AOD underestimation to the boundary layer parameterization and the emissions inventory used for the simulations. Kumar *et al.* (2011) evaluated WRF-Chem's ability to simulate trace gases over the Indian region. They also studied the behaviour of meteorological parameters in this model for 2008 (Kumar *et al.* 2012). Recently, Moorthy *et al.* (2013a) studied the spatio-temporal variation of BC over India using two chemistry transport models, namely, CHIMERE and GOCART. The authors found some discrepancies in the model simulated near-surface BC concentrations in comparison with measurements, for GOCART model and to a lesser extent in CHIMERE model as well. They pointed out the necessary improvements in the boundary layer parameterizations in GOCART model to achieve a better performance in simulating near-surface BC concentrations. However, in most of these studies, the model simulations were compared with measurements made at a few 'spot' locations. In the backdrop of the above, we examine the simulations using a coupled atmospheric chemistry model, WRF-Chem, and evaluate its performance by comparing against ground-based concurrent measurements made at several surface observatories, as well as satellite data. We compare our findings with the earlier reports and discuss the potential causes responsible for the discrepancies between model simulations and the observations. Section 2 outlines the online chemistry-transport model WRF-Chem. Section 3 explains the simulation experiments along with some description of the initial, boundary conditions data and the emissions used in these simulations. In section 4, we present the results of the comparison between the model simulations and different observational datasets, for meteorological parameters and aerosols mass concentrations. Conclusions are presented in section 5.

## 2. WRF-Chem model and simulations

We used online chemistry transport model WRF-Chem (developed at NOAA, National Oceanic and Atmospheric Administration), for the simulations. Detailed documentation of WRF is given in Skamarock *et al.* (2008). It is a nonhydrostatic model and uses Arakawa C-grid. It uses the Runge-Kutta second and third order time-split integration scheme to handle acoustic and gravity-wave modes. The aerosol simulation experiments are performed over the Indian region ( $55^{\circ}$ – $97^{\circ}$ E,  $1^{\circ}$ – $37^{\circ}$ N), for two selected months of May 2011 (pre-monsoon) and October 2011 (post-monsoon).

We used Lambert-conformal projections with the 12 km grid spacing. Thompson scheme (Thompson *et al.* 2004) was used for cloud microphysics and Zhang–McFarlane scheme (Zhang and McFarlane 1995) was used for cumulus parameterization. Boundary layer processes were parameterized using MYJ scheme (Janjić 2002), while RUC–LSM (Smirnova *et al.* 1997, 2000) was used for modelling surface processes. Long and shortwave radiation was computed using RRTMG scheme (Mlawer *et al.* 1997). Both the meteorological and chemistry components use the same transport scheme (mass and scalar preserving), at the same horizontal and vertical resolutions. The chemistry in the simulations is handled using MOZCART chemical mechanism option, which is a combination of MOZART (Emmons *et al.* 2010) mechanisms for gas-phase chemistry and GOCART bulk aerosol scheme (Chin *et al.* 2002) for aerosol phase chemistry, along with Fast-J photolysis scheme (Wild *et al.* 2000). The direct effects of aerosols are taken into account by coupling the aerosol scheme with the radiation scheme.

### 3. Data and methodology

#### 3.1 Initial and boundary conditions for meteorology and chemistry

We have used NCEP FNL (Final) Operational Global Analysis data at 1° interpolated to model resolution to initialize the meteorological variables and for lateral boundary forcing (updated every 6 hours). The initial and boundary conditions for chemistry variables (gases and aerosols) are taken from the global chemistry transport model MOZART4 (Model for Ozone and Related Chemical Tracers, version 4). The standard MOZART4

mechanism includes 85 gas-phase species, 12 bulk aerosol compounds, 39 photolysis, and 157 gas phase reactions. Emmons *et al.* (2010) discusses MOZART4 in detail.

#### 3.2 Emissions

Chemistry-emissions from three different emission inventories have been used, viz., RETRO (Schultz *et al.* 2007), EDGAR (Olivier *et al.* 1996) and GOCART (Chin *et al.* 2002) databases. RETRO provides global emission inventories at 0.5° for different greenhouse and precursor gases. EDGAR provides emissions of primary atmospheric pollutants, CO, NO, SO<sub>2</sub>, NH<sub>3</sub>, and VOCs, gases that contribute to the formation of photochemical smog, inorganic and organic aerosols in the atmosphere. Emissions of aerosol species OC and BC are taken from Goddard Chemistry Aerosol Radiation and Transport (GOCART) database. Table 1 summarizes the use of emission inventories in these model simulations. The actual levels of anthropogenic aerosol emissions over India can be found in table 2.

The emissions of OC and BC are prepared by an emission pre-processor software PREP-CHEM-SRC (version 1). This is one of the standard utilities used in preparing such emissions for WRF-Chem. Freitas *et al.* (2011) discusses this pre-processor in detail. It uses monthly anthropogenic aerosol emissions (OC and BC) at 1° × 1° horizontal resolution from GOCART model database. Details about GOCART can be found in Ginoux *et al.* (2001), Chin *et al.* (2002, 2009). GOCART database follows methodology used in Cooke *et al.* (1999) to develop emission inventory for carbonaceous aerosols.

As such, these emission inventories have some inherent uncertainty. The method employed in Cooke *et al.* (1999) states an uncertainty of factor

Table 1. Emissions' inventories used in the model simulations.

Name of the emissions' inventory	Species
RETRO	Acids, Alcohols, Benzene, Hydrocarbons like C <sub>2</sub> H <sub>2</sub> , C <sub>2</sub> H <sub>4</sub> , etc., Esters, Ketones, Ethers, NO <sub>x</sub> , CO, Methanol and few other species.
EDGAR	CO <sub>2</sub> , SO <sub>4</sub> , CH <sub>4</sub> , N <sub>2</sub> O, SF <sub>6</sub> , etc.
GOCART database	OC, BC, SO <sub>2</sub> (Anthropogenic)

Table 2. Emission levels over India, in these simulations.

Species	Emission levels over southern India	Emission levels over Gangetic plains
BC	0.03 μg m <sup>-3</sup> ms <sup>-1</sup>	0.02–0.08 μg m <sup>-3</sup> ms <sup>-1</sup>
OC	0.2–1.1 μg m <sup>-3</sup> ms <sup>-1</sup>	0.2–1.8 μg m <sup>-3</sup> ms <sup>-1</sup>
SO <sub>2</sub>	4–28 mol km <sup>-2</sup> hr <sup>-1</sup>	4–56 mol km <sup>-2</sup> hr <sup>-1</sup>

of 2 for the inventory. But in general, it is difficult for a country like India to evaluate such an emission inventory, due to lack of observational data of emissions. The validation of these against actual emissions is a mammoth task and is beyond the scope of this work.

### 3.3 Satellite data

#### 3.3.1 TRMM precipitation data

We have used satellite precipitation product 3B42 from TRMM (Tropical Rainfall Measuring Mission) satellite to evaluate simulation of precipitation within the model. The TRMM 3B42 precipitation product has a horizontal resolution of  $0.25^\circ \times 0.25^\circ$ , with a temporal resolution of 3 hours.

#### 3.3.2 TOMS aerosol index data

To understand the annual cycle of aerosol spatial pattern over Indian region, we have utilised a satellite-based aerosol index (AI). AI is a product of Total Ozone Mapping Spectrometer (TOMS) onboard the Earth Probe satellite. It is an index that indicates the presence of UV-absorbing aerosols such as dust and soot, over both land and ocean surfaces. Details about TOMS AI can be found in Herman *et al.* (1997). TOMS AI data from 1996 to 2003 has been used in our study. TOMS AI data has a horizontal resolution of  $1^\circ \text{ lat.} \times 0.8^\circ \text{ long.}$

#### 3.3.3 MODIS aerosol optical depth

We have compared model simulated aerosol optical depths with that from MODIS (Moderate Resolution Imaging Spectro-radiometer). We have used the mean of the following MODIS level 3 products: AOD at 550 nm from TERRA, AOD at 550 nm from Aqua and Deep blue AOD from Aqua (Deep blue TERRA is not available for simulation periods). MODIS AOD data has a resolution of  $1^\circ \times 1^\circ$ . The comparisons are done for monthly mean spatial patterns of AOD during May and October 2011.

### 3.4 Surface observations

Under the Indian Space Research Organization Geosphere Biosphere Program (ISRO GBP), a regional network (ARFINET) of several surface aerosol observatories have been established for near-real time measurements of the mass concentrations of aerosol black carbon (BC) along with other climate parameters (Moorthy *et al.* 2009; Moorthy and Satheesh 2011). In this study, we compare simulated BC mass concentrations with the surface observatories under ARFINET. Data

from following 9 ARFINET observation stations has been used in this study – Bangalore, Chennai, and Trivandrum from southern India; Hyderabad and Ananthpur from central-southern India; Ranchi, Varanasi, and Delhi from northern India; and Dibrugarh from north-east India.

### 3.5 Reanalysis data

We have compared model simulated meteorological parameters like winds (at various pressure levels) and planetary boundary layer height over the region, with that from a reanalysis product MERRA (Rienecker *et al.* 2011) (Modern Era-Retrospective analysis for Research and Applications).

### 3.6 Selection of simulation periods

The model simulations were carried out for the months of May and October 2011. An examination of the 8 years averaged TOMS aerosol index over India (figure 1) reveals a peak in May, a strong reduction during monsoon months (JJAS) and reduced AI during October. During May, dust is advected by prevailing north-westerly winds into India (especially into the Indo-Gangetic Plains, IGP) from Sindh and Arabia (Lau *et al.* 2006). This dust combines with local black carbon emissions from the IGP and causes AI to be high. During monsoon season, rains scavenge a large fraction of dust and a lesser fraction of BC and AI is low (figure 1b). Post-monsoon (dry season, winter-time, after October), BC over IGP builds up due to lack of wet scavenging and due to near-stable atmospheric condition and causes AI to be higher. Hence, we chose May 2011 and October 2011 as representative periods for analysis, to capture the pre-monsoonal peak and the post-monsoonal minima in AI.

### 3.7 Methodology

We have evaluated the performance of the model WRF-Chem in simulating meteorological parameters and aerosol mass concentrations over the Indian region ( $55^\circ\text{--}97^\circ\text{E}$ ,  $1^\circ\text{--}37^\circ\text{N}$ ) for two representative months, viz., May 2011 (pre-monsoon period) and October 2011 (post-monsoon period). Additionally, simulations were conducted for March 2006 and January 2009 for the comparison of vertical profiles with aircraft observations that were available for these periods as part of the ICARB (Integrated Campaign for Aerosols, Gases and Radiation Budget) (Moorthy *et al.* 2008) and W-ICARB (Winter Integrated Campaign for Aerosols gases and Radiation Budget) (Moorthy

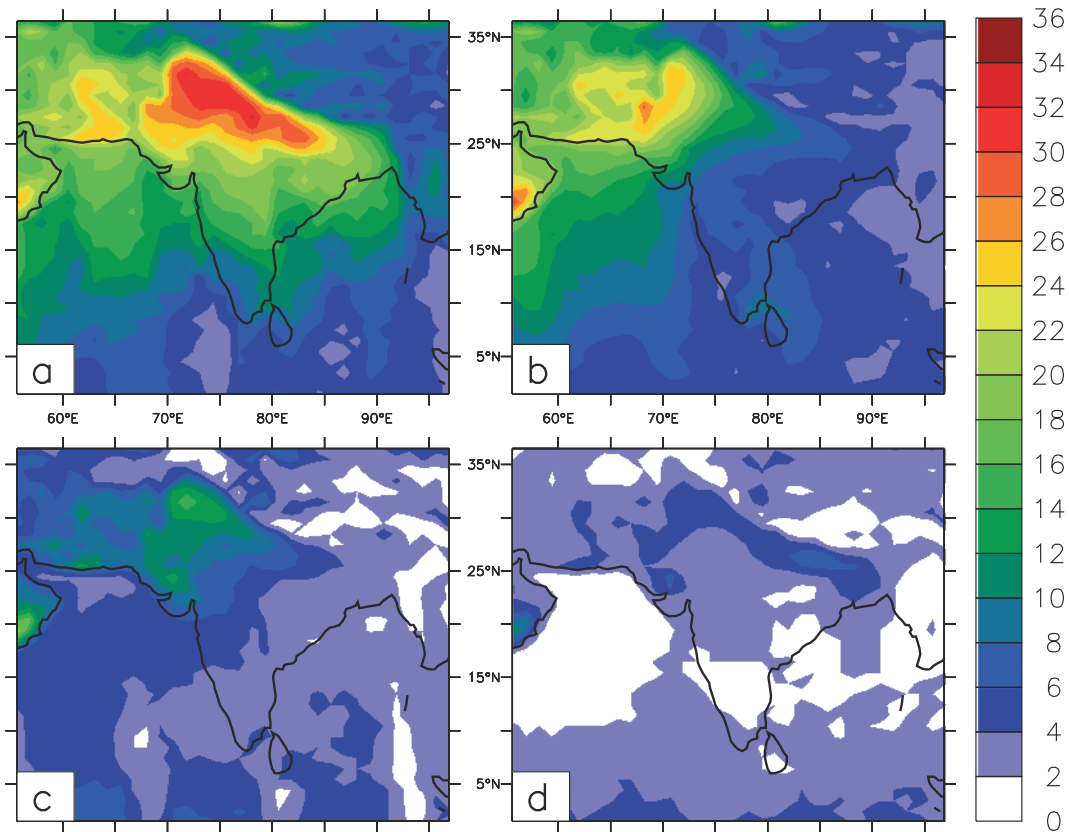


Figure 1. Spatio-temporal variation of TOMS aerosol index (AI) averaged over a period of 1996–2003, over Indian region. Figure shows the values of  $(AI \times 10)$ , for (a) May, (b) JJAS mean, (c) October and (d) December.

*et al.* 2010; Sreekanth *et al.* 2011) campaigns. Initial spin up does not seem to have a significant impact on the simulations. The simulated atmospheric state variables (wind, rainfall, and planetary boundary layer height) are compared with reanalysis dataset and satellite data. The model simulated aerosol optical depths are compared with MODIS (mean of Terra + Aqua) dataset.

## 4. Results and discussions

Before we proceed using the model simulation for aerosols, it is essential to examine its capability to reproduce the regional meteorology over the domain and its seasonality.

### 4.1 Evaluation of simulated meteorological parameters

Meteorological conditions influence overall aerosol concentrations (Sánchez-Ccoyllo O and de Fátima Andrade 2002; Wehner and Wiedensohler 2002; Jones and Harrison 2004; Satheesh and Moorthy 2005) through transport, scavenging and mixing of aerosols within atmosphere and therefore, errors in meteorological simulations could lead to errors

in estimating aerosol concentrations. Therefore, it is important to compare WRF-simulated atmospheric state variables with those from reanalysis and satellite-derived data.

#### 4.1.1 Wind

In figure 2, we compare monthly mean model-simulated wind fields over the Indian region with MERRA (Rienecker *et al.* 2011), for May and October 2011. Model simulations were re-gridded to MERRA resolution of  $(1/2)^\circ$  lat.  $\times$   $(2/3)^\circ$  long. for comparison. Though we compared winds at three different pressure levels (850, 500, and 200 hPa), here we present results only for 850 hPa (figure 2).

During May 2011, at 850 hPa, MERRA (figure 2a) shows a north-westerly wind pattern over the Indian landmass, a south-westerly wind pattern over Bay of Bengal, a south-west to north-west curling tendency over Arabian Sea, and a cyclonic tendency over north of Bay of Bengal. These features are realistically simulated by the model (figure 2b). However, the anticyclonic flow over central Arabian Sea observed in MERRA in May 2011 is less discernible in the simulation. During October 2011, it is seen that MERRA

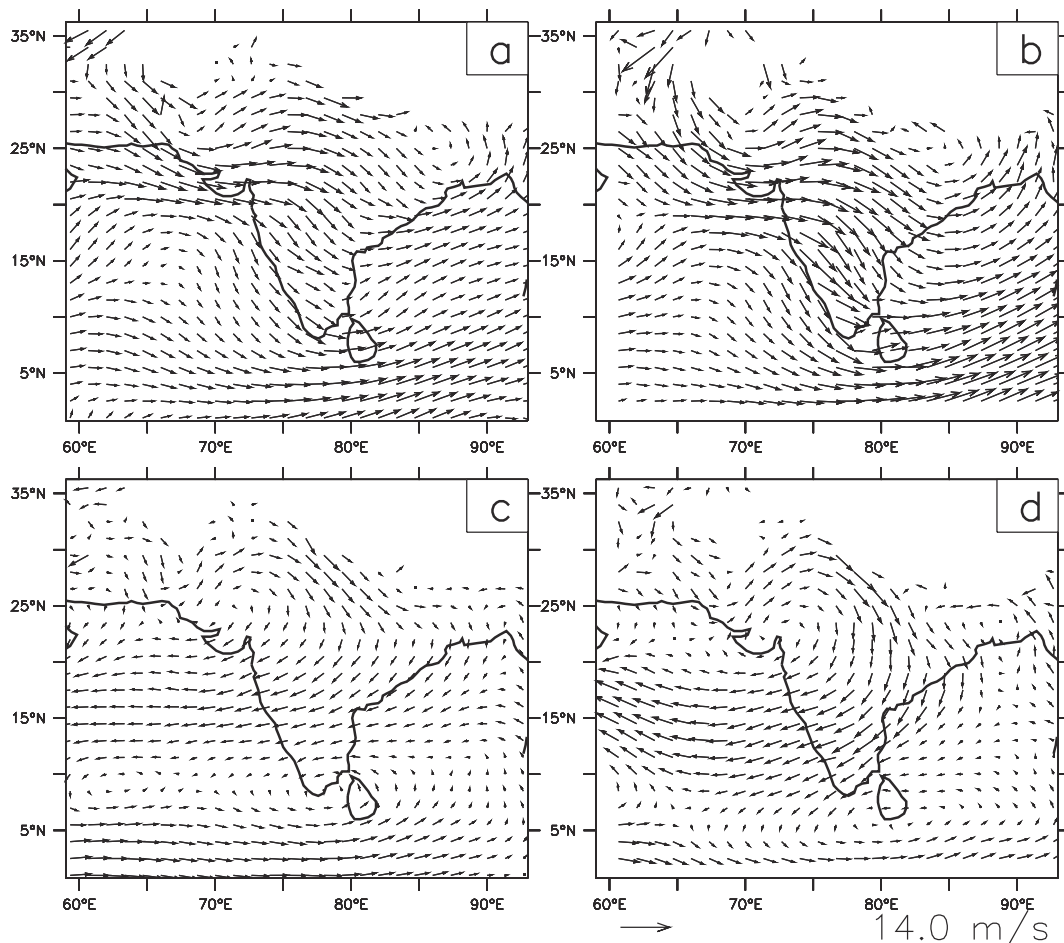


Figure 2. Monthly mean horizontal wind patterns at 850 hPa over Indian region for (a) May 2011, from MERRA, (b) May 2011, from model, (c) October 2011, from MERRA, and (d) October 2011, from model.

(figure 2c) shows an anticyclonic tendency centered over north-western India; while the Gangetic plains seem to have north-westerly winds, and northern Bay of Bengal and central India have north-easterly flows. Model simulations (figure 2d) show most of the features of the wind pattern with an anticyclonic pattern over north-western India and north-westerlies over the Gangetic plains. However, model's simulation of flow over western Arabian Sea is less realistic. Thus with a few exceptions, model realistically simulates wind pattern over the region. Similar behaviour is noticed at 500 and 200 hPa (figures not shown).

Wind speed and its regional pattern have influence in the transport of aerosol species, so it is important to evaluate model's performance in capturing the wind magnitudes. To quantify model's performance in simulating wind speeds over the region, our complete domain is divided into eight different regional boxes (figure 3). An 'adjustment factor', defined as the ratio of model's monthly mean wind speed to MERRA monthly mean wind speed averaged over the corresponding region is estimated for each region and listed in table 3. It is

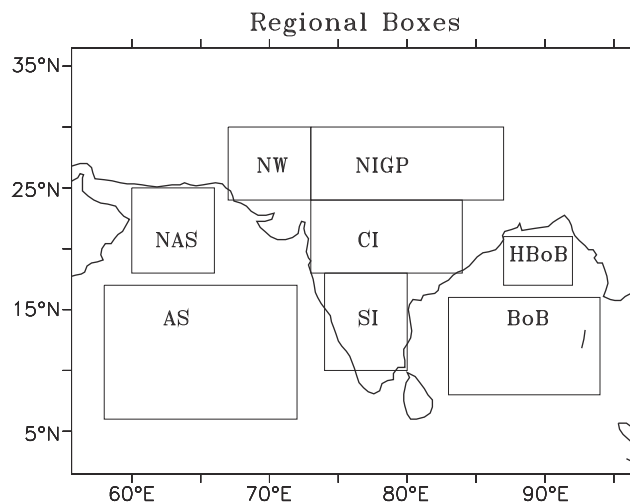


Figure 3. The different regional boxes into which the complete domain is divided to calculate the adjustment factors, in this study.

seen that the model overestimates the wind speed over the landmass (top 4 rows, table 3), for both the months while the model's performance in simulating wind speed over the oceanic bodies (last

4 rows, table 3), in contrast, seem to change drastically from May to October. While it overestimates winds over BoB in May, an underestimation is seen in October. Similar contrasting behaviour for May and October is seen over Arabian Sea. However, temporal variation of wind speed over northern Bay of Bengal are realistically simulated *vis-a-vis* MERRA (as can be seen from high correlations in table 3) while the magnitudes are overestimated. Over the Indian landmass also, there is good temporal correlation between model and MERRA (the exceptions being northwestern India in May and central India in October). In summary, model

simulates the spatial and temporal pattern of wind speed variations realistically but the magnitudes are somewhat overestimated.

#### 4.1.2 Rainfall

We compare monthly model simulated rainfall with that from TRMM for May and October 2011. During May 2011, over the Indian landmass, TRMM (figure 4) shows highest rainfall (0.6–0.8 mm/hr) over the north eastern region, followed by the foothills of Himalayas, the eastern coast, and

Table 3. Adjustment factors (AF) between model wind speed and MERRA wind speeds, averaged over the selected regions, for both the months. CC=correlation coefficient between model and MERRA, AF=(model value/MERRA value) significance levels for CC: NW in May: 98%, CI in Oct: 40%, Rest all: >99%.

Area	Region	May AF	Oct AF	CC, May	CC, Oct
North India and Gangetic plains	73°–87°E, 24°–30°N	1.07	1.23	0.61	0.59
Northwestern India	67°–73°E, 24°–30°N	1.22	1.47	0.28	0.47
Central India	73°–84°E, 18°–24°N	1.53	1.21	0.69	–0.06
Southern India	74°–80°E, 10°–18°N	1.47	1.67	0.65	0.87
Bay of Bengal	83°–94°E, 8°–16°N	1.59	0.8	0.8	0.92
Head Bay of Bengal	87°–92°E, 17°–21°N	1.08	1.02	0.67	0.45
Arabian Sea	58°–72°E, 6°–17°N	1.1	1.59	0.88	0.77
North Arabian Sea	60°–66°E, 18°–25°N	1.11	0.79	0.59	0.29

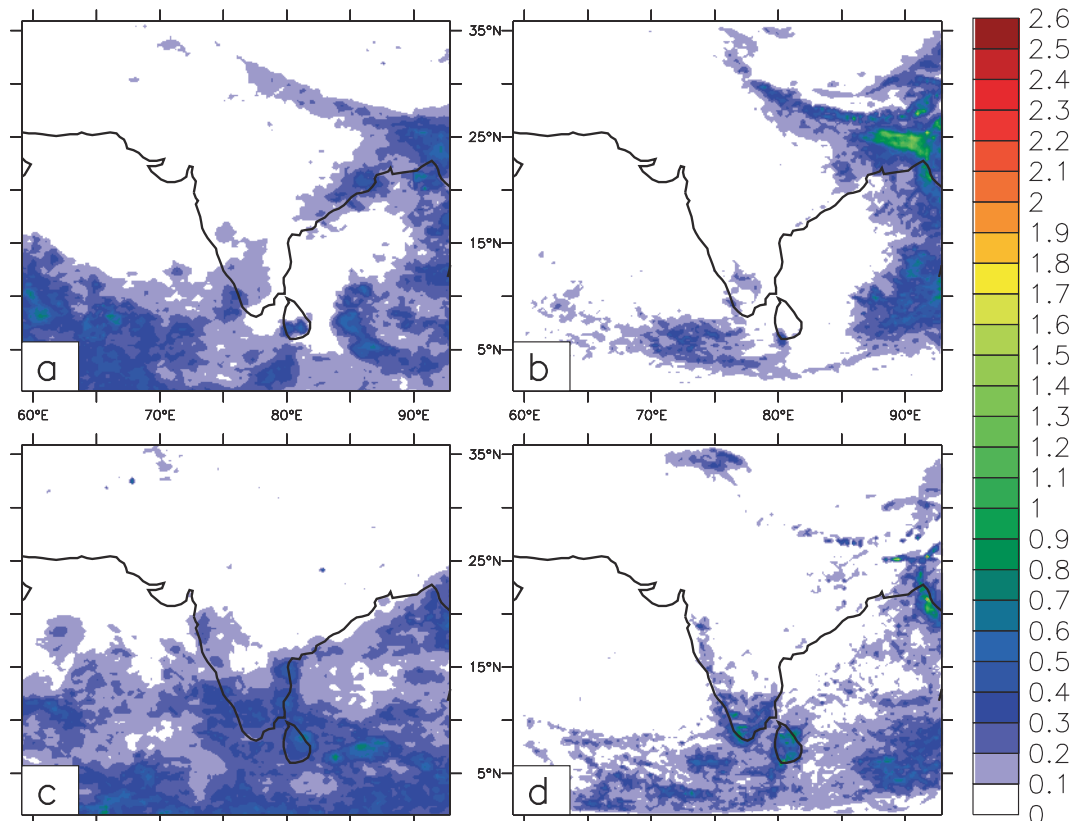


Figure 4. Monthly mean total precipitation (mm/hr) over Indian region for (a) May 2011, from TRMM, (b) May 2011, from model, (c) October 2011, from TRMM and (d) October 2011, from model.

southern central India with values 0.1–0.4 mm/hr. Over Bay of Bengal and central and southern parts of Arabian Sea, TRMM shows rainfall values ranging from 0.2–0.5 mm/hr. For the same month, model simulations (figure 4b) show highest rainfall values (1–1.4 mm/hr) over northeast part of India, 0.1–0.6 mm/hr from north of Bay of Bengal to Himalayan region, 0.1–0.2 mm/hr for some part of southern India. Model simulations show values ranging from 0.2–0.6 mm/hr over eastern part of Bay of Bengal; southeast Arabian Sea is seen with values ranging from 0.2–0.4 mm/hr in model simulations. Thus the model simulates high rainfall over NE India and eastern Bay of Bengal realistically but fails to simulate the higher rainfall over central-southern Arabian Sea and parts of eastern coast of India.

During October 2011, TRMM (figure 4c) shows high rainfall over Western Ghats, southern peninsula, central and southern parts of Arabian Sea, and over entire Bay of Bengal. The values range from 0.2–0.7 mm/hr over these regions. Model (figure 4d) shows higher rainfall values ranging from 0.2–0.5 mm/hr, over Western Ghats, southern part of India, Bay of Bengal (scattered patches), Himalayan region and over southern part of Arabian Sea. Model shows highest rainfall (0.8–1.2 mm/hr) over southern India, Sri Lanka, and northeast India and Myanmar. The simulations show a reasonable agreement with TRMM over most of the Indian region (except for a few places over the eastern coast), but rainfall over central Arabian Sea is underestimated. We find that Root Mean Square Error (RMSE) of monthly mean model simulations *vis-a-vis* TRMM is 0.14 mm/hr for May and 0.1 mm/hr for October, with a higher agreement over land regions. Thus, the model reasonably simulates the monthly mean rainfall

pattern over the Indian landmass – the region of interest of our present work. We have also made a comparison between time series of 3-hourly rainfall from model with that from TRMM, for a few stations, viz., Bangalore and Kolkata (figure 5). We found that while the model captures the monthly mean rainfall reasonably well, the phase and intensity of the rain events at smaller scales are not well simulated.

#### 4.1.3 Planetary boundary layer (PBL) height

The variations in surface aerosol concentration depend on several factors including source strengths, microphysics, and ventilation within atmosphere, in addition to temperature and RH. The meteorological factors influence the aerosol concentration at any location through redistribution (both horizontal and vertical, respectively through advection and convective eddies) and removal mechanisms. In this context, the height of the planetary boundary layer is important as it is one of the factors that determines the extent of aerosol mixing that can occur in the vertical and plays an important role in redistribution (e.g., Nair *et al.* 2007).

We compared monthly mean PBL heights simulated by the model with those from MERRA, for the two months under consideration. During May 2011 (figure 6a), MERRA shows higher PBL heights over the central and northern parts of India (regions where the solar radiation is intense and strong thermal convections are present during this month) as compared to the southern part. Model simulations for May 2011 (figure 6b) do not show such a difference in PBL heights over the southern and northern parts of India and could be related

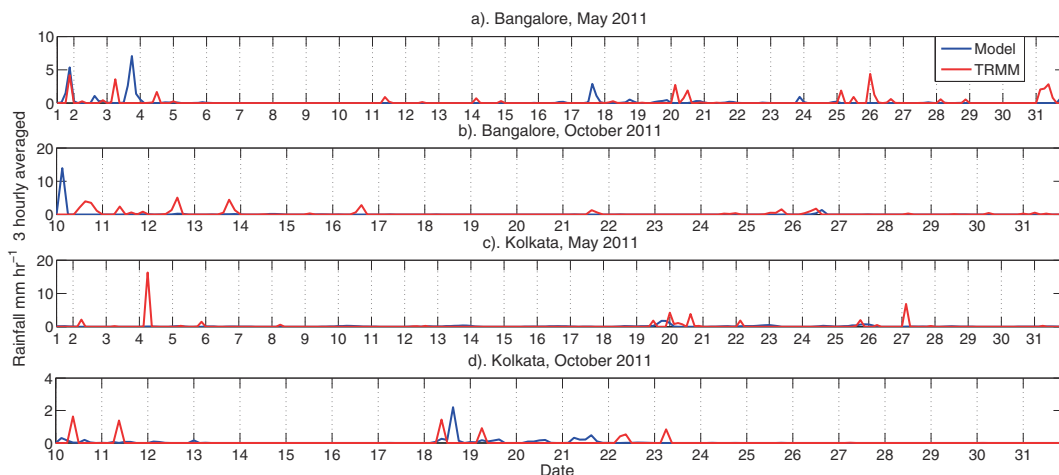


Figure 5. Time-series of rainfall over Bangalore for (a) May 2011, (b) October 2011; over Kolkata for (c) May 2011 and (d) October 2011.



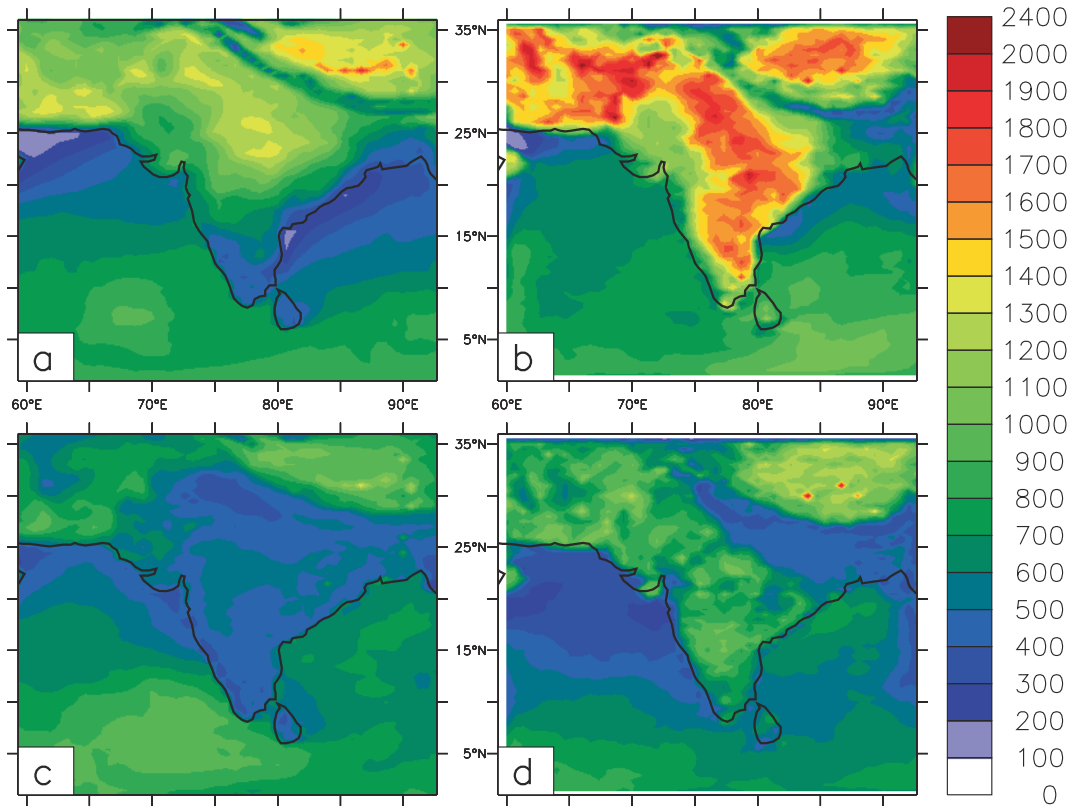


Figure 6. Monthly mean spatial variation of Planetary Boundary Layer (PBL) height (m) over the study region for (a) May 2011, from MERRA, (b) May 2011, from model, (c) October 2011, from MERRA and (d) October 2011, from model.

Table 4. Adjustment factors (AF) between model PBL heights and MERRA PBL heights, averaged over the selected regions, for both the months.  $AF = \text{Model value} / \text{MERRA value}$ .

Area	Region	May AF	October AF
North India and Gangetic plains	73°–87°E, 24°–30°N	1.25	1.22
Northwestern India	67°–73°E, 24°–30°N	1.39	1.48
Central India	73°–84°E, 18°–24°N	1.63	1.52
Southern India	74°–80°E, 10°–18°N	2.19	1.51
Bay of Bengal	83°–94°E, 8°–16°N	1.37	0.86
Head Bay of Bengal	87°–92°E, 17°–21°N	1.50	0.98
Arabian Sea	58°–72°E, 6°–17°N	0.98	0.71
North Arabian Sea	60°–66°E, 18°–25°N	1.67	0.64

to lack of rainfall over southern peninsula during May in the model simulation. During October, PBL gets shallower (figure 6c and d) due to relatively stable atmospheric conditions. Model simulations (figure 6b and d) overestimate the PBL heights as compared to MERRA (figure 6a and c) for both the months, with a few exceptions like Himalayan region and Indo-Gangetic plains for October 2011 (figure 6d). We quantify the mismatch for the same boxes (figure 3) by calculating the adjustment factors between model values and corresponding MERRA values (table 4). It is clearly seen that, model overestimates the PBL

heights over the land regions for both the months (first 4 rows, table 4). Over the oceanic regions (last 4 rows, table 4), model's performance is better in the month of October (4th column) than that in May (3rd column), with exception of Arabian Sea. Deeper boundary layer could lead to higher vertical mixing and hence lower aerosol concentration at the surface. This is discussed further in section 4.3.1.

Additionally, we have compared model simulated specific humidity and relative humidity with that from MERRA (figures not shown). It is seen that, while the model satisfactorily simulates specific

humidity over most part of the land mass (except Gangetic plains), it does an overestimation over the oceans, at 925 hPa level. The vertical profiles of model simulated relative humidity over different grid boxes across the region do not match with the corresponding profiles from MERRA (figure not shown).

#### 4.2 Simulated aerosol parameters

In this section, we present the results of simulation of optical depth and the mass concentrations and compare these with measurement.

##### 4.2.1 Aerosol optical depth (AOD)

The most important parameter to represent the climate impact of aerosols is spectral aerosol optical depth (AOD), which is the vertical integral, through the entire height of the atmosphere, of the fraction of incident light as a function of wavelength, scattered and/or absorbed by aerosols. For evaluating the model's performance in simulating the column aerosol concentrations, we have used monthly mean AOD (550 nm) derived from the model results, along with that retrieved from MODIS (Aqua+Terra). We compared model AOD

at 550 nm with the mean of (MODIS Aqua (550 nm), MODIS Terra (550 nm), MODIS Deepblue Aqua (MODIS Deepblue Terra has no valid data over the region for that period)). This kind of averaging of MODIS products is done to reduce the total number of missing patches in MODIS AOD.

Notwithstanding the known uncertainties of satellite-derived AODs over heterogeneous land-mass (Remer *et al.* 2005; Zhang *et al.* 2005; Kahn *et al.* 2007; Levy *et al.* 2010) it is seen that for the month of May 2011, MODIS shows highest values (0.65–0.9) of AOD over the Indo-Gangetic plains (figure 7a). This is attributed to the dust loading from deserts of Arabia and north western India (Moorthy *et al.* 2007) and mixing of this dust with local anthropogenic emissions. High values of aerosol optical depth over the coasts of India (0.6–0.7 over east coast and 0.5–0.6 over the west coast) could be due to the presence of sea-salt aerosols, dust (over west coast) and other anthropogenic aerosols (over the area near eastern coast of India). Model simulations of the spatial distribution of AOD at 550 nm for the same period (figure 7b) show higher AOD values (0.45–0.55) over Gangetic plains and eastern coast of India; however, the magnitudes are comparatively lower than that of MODIS. Model shows relatively lower

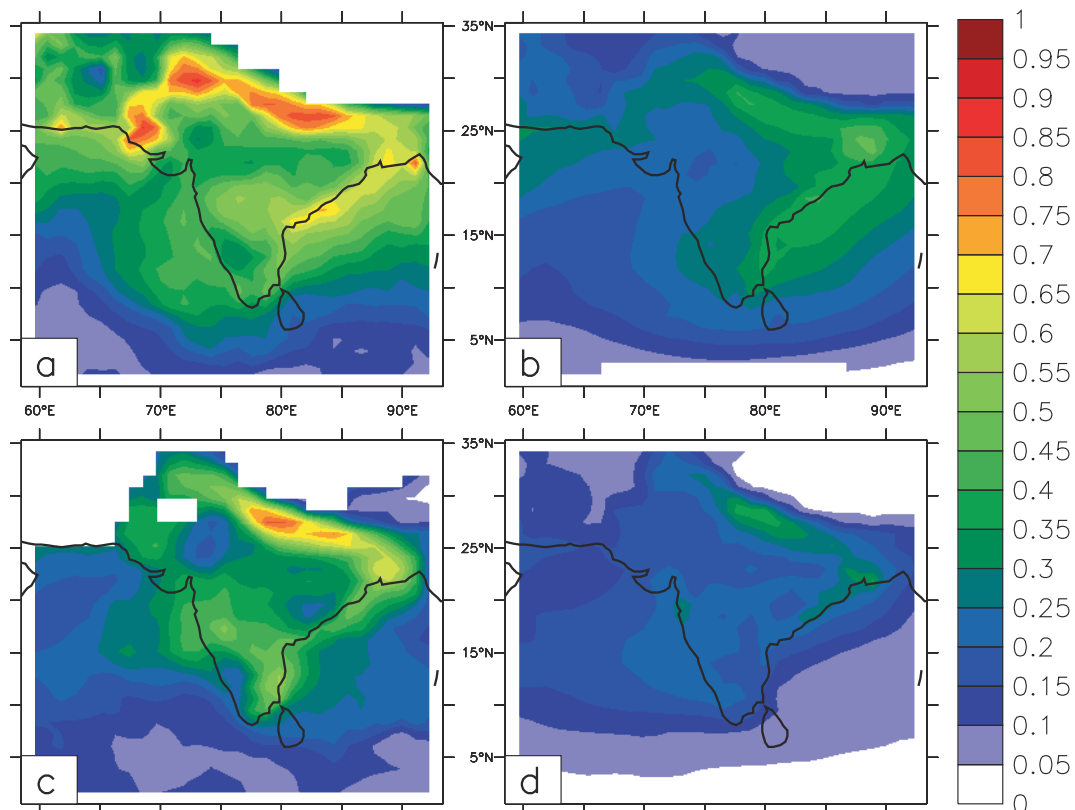


Figure 7. Monthly mean spatial distribution of aerosol optical depth (AOD) at 550 nm, over Indian region for (a) May 2011, from MODIS, (b) May 2011, from model, (c) October 2011, from MODIS, and (d) October 2011, from model.

values over central and western parts of India, and successfully simulates the higher AOD over north-western parts (than over central India). However, model fails to simulate the relatively higher AOD values over northern Bay of Bengal. Thus while the model captures the spatial pattern of AOD it underestimates the magnitudes for May 2011.

During October 2011 (figure 7c), MODIS shows a moderate AOD over the north Indian region as compared to May (figure 7a); yet the highest AOD (0.65–0.8) occurs over the Gangetic plains (comparable to May), followed by eastern coast (0.45–0.65), with central India showing minimum values (0.25). Model (figure 7d) also does simulate the reduction in overall AOD values as compared to May (figure 7b), with higher AODs over Gangetic plains (0.4–0.5) and over Bengal and central-western coast. For the rest of the domain, it shows values lesser than 0.3. Except over north-western India and Sindh, model simulates a similar pattern as that of MODIS even though the magnitudes are largely underestimated by the model during October 2011. Thus, while reasonably replicating the monthly mean spatial distribution pattern, the model underestimated the magnitude of AOD during both the months.

With a view to quantify this underestimation we calculated the ‘Adjustment Factor’ (AF), i.e., the ratio of the observed (MODIS) AOD to the model simulated AOD, for all the eight different regions (figure 3) for the regional mean values of AOD, and the same are listed in table 5. It is seen that the model largely underestimates the AOD for both the months over the complete region with AF values going as high as  $\sim 3$  (table 5, columns 5 and 8). For both the months, larger AF values are seen over land than that over ocean; with an exception of Bay of Bengal in October (where  $AF_{\text{ocean}}$  is larger than  $AF_{\text{land}}$ ). The higher values of AF over land could be due to the uncertainty with satellite retrievals of AOD over land. MODIS tends to overestimate AOD over land surface (Jethva *et al.* 2007, 2009).

Model’s performance over land gets improved in October *vis-a-vis* May, except for SI. For oceans, model performs better over BoB in May than in October and *vice-versa* for AS. Thus, the model underestimates AOD magnitudes while reproducing the AOD pattern *vis-a-vis* MODIS. The mean ratio between model AOD and observed AOD for the total Indian region is 1.7 during May and 1.85 during October.

#### 4.2.2 Surface black carbon (BC) mass concentration

Evaluation of model for BC concentrations and its spatio-temporal variability is another important step mainly due to the strong radiative effects of BC (specifically, absorption of incoming solar and outgoing longwave radiation). Though the radiative effects of BC are more effective in middle to upper atmosphere, we compare the model simulated BC mass concentration values at surface level with the corresponding surface observational values, mainly due to the fact that, we do not have a continuous upper air BC measurement data. We have compared the model simulations with the data from ARFINET observations for nine stations across India, for the two months. The scatter plots are shown for 6-hourly BC data from the model and the observational sites (figure 8a–d). Over Bangalore (in south central peninsula), for May 2011 (figure 8a) model underestimates the BC concentrations, with a mean adjustment factor of 2.63 ( $AF = \text{Observed BC} / \text{Model BC}$ ). Similar underestimations of BC mass concentrations by the model are seen for Trivandrum (figure 8c) as well ( $AF$  close to 3.2). For Chennai (another urban conglomeration in the eastern peninsula) in the month of October (figure 8b), the observed BC values are as high as  $23 \mu\text{g m}^{-3}$ , while the model peak is only about  $7 \mu\text{g m}^{-3}$ , the mean AF value being more than 5, while at Delhi for May (figure 8d), with

Table 5. Adjustment factors between model simulated values of aerosol optical depth at 550 nm, with the corresponding values from MODIS satellite data, for May and October 2011:  $AF = \text{MODIS AOD} / \text{Model AOD}$ .

Area	Region	MODIS, May	Model, May	AF May	MODIS, Oct	Model, Oct	AF Oct
North India and Gangetic plains	73°–87°E, 24°–30°N	0.51	0.27	1.88	0.37	0.21	1.76
Northwestern India	67°–73°E, 24°–30°N	0.6	0.25	2.4	NA	0.2	NA
Central India	73°–84°E, 18°–24°N	0.43	0.25	1.72	0.31	0.2	1.55
Southern India	74°–80°E, 10°–18°N	0.44	0.29	1.52	0.4	0.2	2
Bay of Bengal	83°–94°E, 8°–16°N	0.33	0.26	1.27	0.24	0.07	3.42
Head Bay of Bengal	87°–92°E, 17°–21°N	0.56	0.35	1.6	0.36	0.17	2.11
Arabian Sea	58°–72°E, 6°–17°N	0.27	0.17	1.59	0.19	0.17	1.12
North Arabian Sea	60°–66°E, 18°–25°N	0.41	0.25	1.64	0.21	0.14	1.5

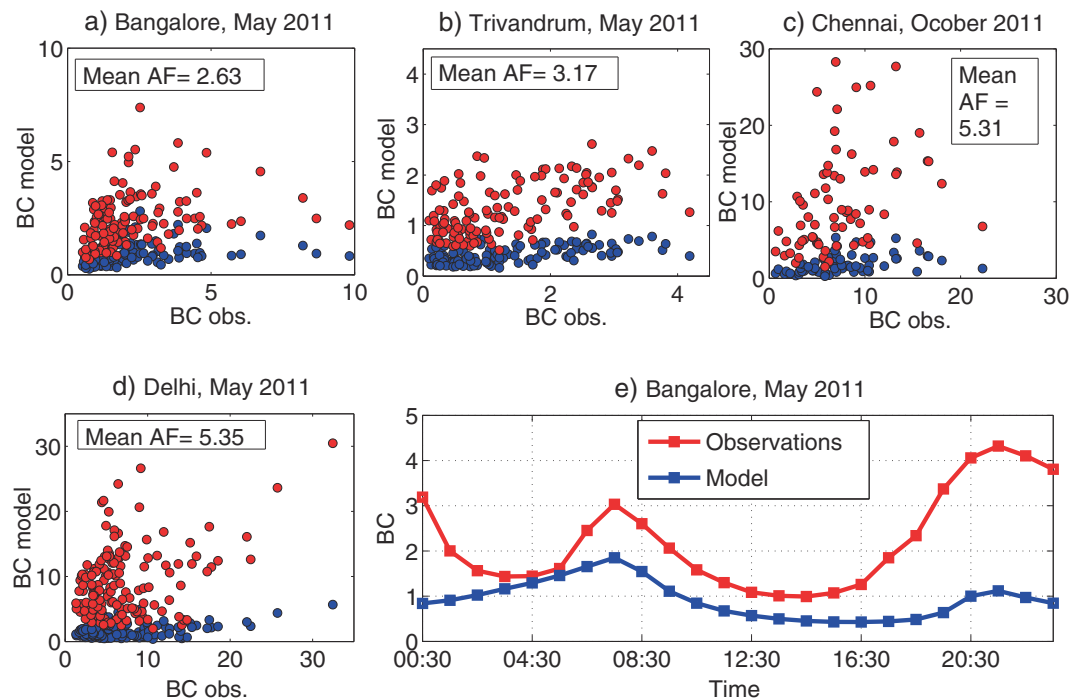


Figure 8. Scatter plots between surface BC mass concentration by WRF-Chem model simulations and station observational data over (a) Bangalore, for May 2011, (b) Trivandrum, for May 2011, (c) Chennai, for October 2011, and (d) Delhi, for May 2011. All the BC values are in  $\mu\text{g m}^{-3}$ , scatter points between the actual model values and the observations are in blue, and scatter points between model values  $\times$  mean AF values and the observations are in red. (e) Monthly mean diurnal variation of surface mass concentration of BC over Bangalore, for May 2011.

Table 6. Adjustment factors between model simulated values of monthly mean near-surface black carbon mass concentration, with the corresponding values from station observational data, for May and October 2011.

Station	Month	Observation BC ( $\mu\text{g m}^{-3}$ )	Model BC ( $\mu\text{g m}^{-3}$ )	Adjustment factor
Bangalore	{ May	2.42	0.92	2.63
	{ October	2.378	2.626	0.91
Chennai	{ May	4.380	2.055	2.13
	{ October	7.61	1.9	4.00
Trivandrum	{ May	1.35	0.421	3.21
	{ October	2.286	0.528	4.33
Hyderabad	{ May	4.251	1.69	2.66
	{ October	4.133	2.899	1.42
Ananthpur	May	2.937	0.796	3.69
Ranchi	May	3.973	1.837	2.16
Varanasi	{ May	4.725	2.447	1.93
	{ October	12	4.243	2.83
Delhi	May	7.05	1.73	4.07
Dibrugarh	{ May	4.956	1.347	3.68
	{ October	3.436	1.53	2.45

observational maxima of about  $30 \mu\text{g m}^{-3}$ , whereas the model maxima is about  $7 \mu\text{g m}^{-3}$ , the AF being higher than 5. Additionally, such comparisons are done over five more stations, viz., Hyderabad (urban, central-south India,  $78.47^\circ\text{E}$ ,  $17.36^\circ\text{N}$ ), Ananthpur (semi-urban, central-south India,  $77.6^\circ\text{E}$ ,

$14.68^\circ\text{N}$ ), Varanasi (semi-urban, north India,  $82.95^\circ\text{E}$ ,  $25.28^\circ\text{N}$ ), Ranchi (semi-urban, north India,  $85.33^\circ\text{E}$ ,  $23.35^\circ\text{N}$ ) and Dibrugarh (semi-urban, northeast India,  $95^\circ\text{E}$ ,  $27.48^\circ\text{N}$ ). The results of all those comparisons can be seen in table 6.

We have also constructed the monthly mean diurnal cycle (hourly data) for surface BC concentrations over Bangalore, from observations and model simulations, for May 2011 (figure 8e). It can be seen from the time-series (figure 8e) that, observations (red) show a 2-peak behaviour, with a morning peak around 7:30 (all times are in IST) (due to traffic and fumigation effect in which the particles in the entrainment zone enter into the boundary layer as the morning rise in inversion occurs) and an evening peak around 21:30 (due to traffic, and the formation of the shallow nocturnal boundary layer, which confines the local emissions, suppressing the vertical dispersion that was active during the well-developed convective conditions during the daytime). Observations (red) show the minima for BC around 4:00 (due to reduced emissions) and around 14:30 (due to highly mixed boundary layer). Model (blue) shows a bi-modal behaviour with a morning peak at about 7:30 and evening peak at about 21:30. Model minima occurs around 17:30 and 00:30. Model simulations also appear to be strongly influenced by meteorological effects (such as boundary layer height) as the specified emissions do not incorporate a diurnal cycle. Except during midnight hours, model's diurnal cycle of BC concentrations is similar to that in observations. Thus, model systematically underestimates BC concentrations as compared to observations, which is apparent in the surface BC time-series comparison over different stations (figure 9a–c) while reproducing the diurnal pattern, in general. It can also be seen from the time-series plots (figure 9a–c) that, the model simulates the diurnal variation in the concentration, but it does not simulate the changes that occur in the

daily maxima of BC as compared to that in the observations.

Comparing observations with model simulated surface BC concentration (figure 8a–d), we notice that a single value of adjustment factor cannot be computed at 6-hourly and daily time-scales, for the complete domain. It can be seen that (table 6), on the monthly mean basis, the adjustment factor between the observations of surface BC mass concentrations and that from the model simulations ranges from 0.9 to 4.3 for the available observational sites.

#### 4.2.3 Vertical profile of BC mass concentration

Vertical distribution of BC affects the moist static energy in lower troposphere (Chakraborty *et al.* 2004). Atmospheric heating due to BC absorption can perturb the large scale of Indian Summer Monsoon Rainfall (Lau *et al.* 2006; Wang *et al.* 2009; Tao *et al.* 2012). In this section, we present the discussion on evaluation of model simulated vertical profiles of BC. The vertical profiles of BC from model over a few stations are compared with the measurements that are taken from aircraft. Sorties over these locations were carried out as a part of the ICARB (Moorthy *et al.* 2008 for details) and W-ICARB (Moorthy *et al.* 2010; Sreekanth *et al.* 2011) campaigns under the Geosphere Biosphere Programme of the Indian Space Research Organization (ISRO-GBP). For comparison we have run WRF-Chem for the periods of observation in March 2006 and January 2009 and the same are presented here.

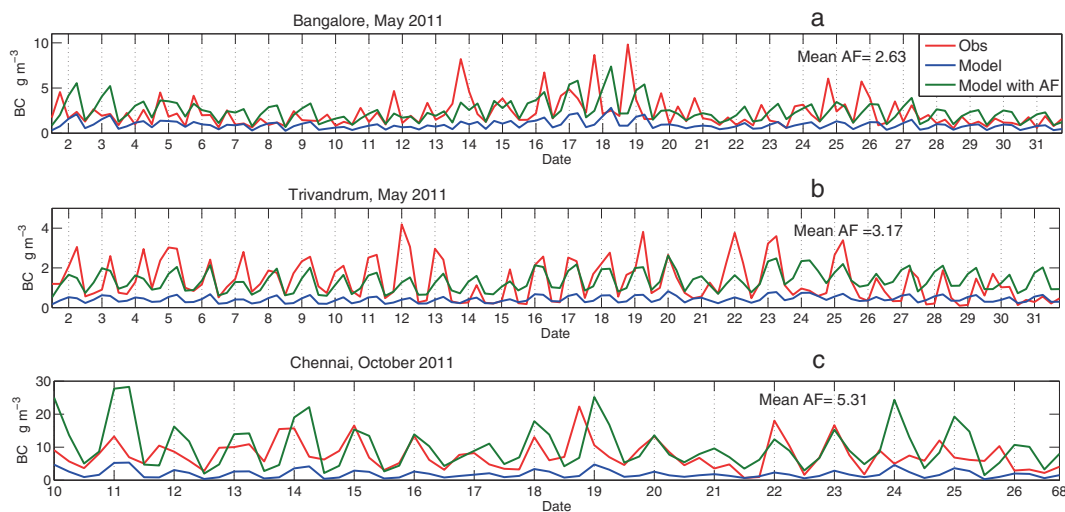


Figure 9. Time series of BC mass concentration from model simulations and stations observations 6 hourly data over (a) Bangalore, for May 2011, (b) Trivandrum, May 2011, (c) Chennai, for October 2011. Observational BC values are in red, Model BC values are in blue and Mean AF  $\times$  model BC values are in green.

We compare model simulated vertical profile of BC with that obtained from ICARB data (figure 10a) and W-ICARB data (figure 10b and c). Over Bhubaneswar (figure 10a), situated on the eastern coast of India, it can be seen that, model simulated vertical profile of BC above 500 m from ground is similar to the observed BC vertical profile, but there is a systematic underestimation by about a factor of 3. For the same station (figure 10a), model realistically simulates the increasing trend between 500 and 1000 m possibly due to advection of BC from the surrounding region. But model's boundary layer processes appear to over-mix the near-surface BC within the boundary layer over the station, thus failing to get the vertical profile similar to observations, below 500 m. For Hyderabad, a station in south central India (figure 10b), the model increasingly underestimates BC above 1 km. For Hyderabad (figure 10b), model is not able to simulate the sharp reduction in BC away from the surface within the boundary layer. This appears to be again associated with the model's overestimation of boundary layer height resulting in higher mixing of particulates within the lower atmosphere, providing larger volume for near-surface BC to disperse vertically, giving a lesser reduction in BC concentration away from the surface within the lower troposphere. Over Port Blair (an island in eastern part of Bay of Bengal) and Visakhapatnam (a station over eastern coast of India, VSK), the vertical profiles of BC (figure 10c) as given by model and aircraft observations show a better agreement. Over Port Blair, there appears to be an underestimation at higher levels possibly

due to underestimation of long-range transport from south-east Asia. The mismatch between BC profile over VSK, is very similar to that at Hyderabad (figure 10b), it hints at possible underestimation of emissions and also to higher boundary layer mixing within PBL in model simulations. Overall, the comparison of vertical profiles of BC over the stations shows a systematic underestimation of BC which could be attributed to the improper emissions; and a relatively steady BC concentration within the boundary layer *vis-a-vis* observations, which could be attributed to a stronger vertical mixing within the boundary layer.

#### 4.3 Potential causes for the discrepancies between model simulations and observations

From the discussions in the previous sections, it is clear that the model WRF-Chem underestimates aerosol mass concentrations and their optical effects (AOD) over the Indian region as compared to observations from surface observatories of ARFINET, satellite data and aircraft measurements. Possible causes for this systematic discrepancy could be:

1. Use of incorrect emissions and initial conditions of BC for the simulations.
2. Increased scavenging of BC due to unrealistic simulations of rainfall by the model as compared to observations.
3. Limitations of model aerosol-chemistry.
4. Incorrect simulations of vital meteorological parameters (wind, PBL heights).

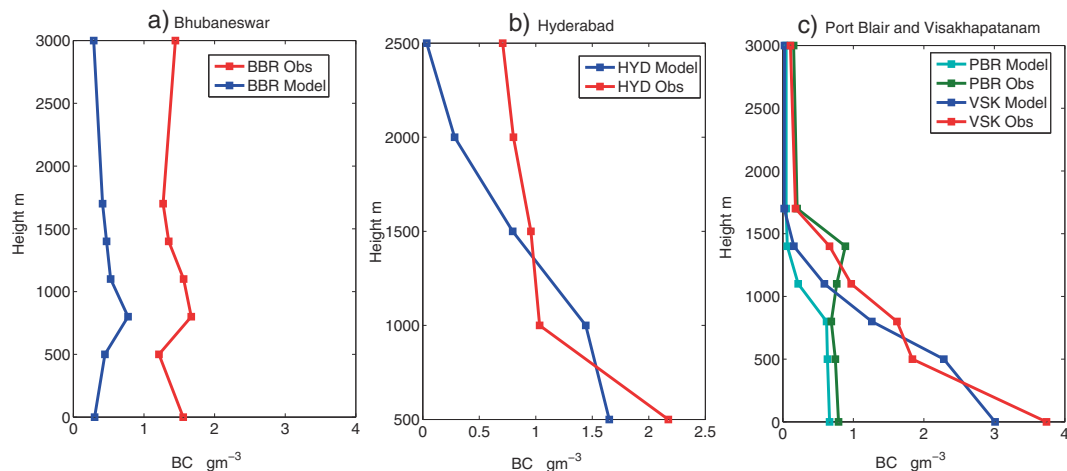


Figure 10. (a) Vertical profiles of BC mass concentration over Bhubaneswar (20.27°N, 85.84°E) on 28th March 2006 from 9:30 to 12:30 local time during ICARB campaign. (b) Vertical profiles of BC over Hyderabad (17.45°N, 78.45°E) on 2nd January 2009 from 10:30 to 14:00 local time during W-ICARB campaign. (c) Vertical profiles of BC over Port Blair or PBR (11.7°N, 92.78°E) on 12th January 2009 from 6:30 to 9:30 local time and over Visakhapatnam or VSK (17.7°N, 83.2°E) on 4th January 2009 from 9:30 to 13:30 local time during W-ICARB campaign.

We analyse these factors in the following part. We confine our analysis to the impact of meteorological parameters in the present study.

#### 4.3.1 Effect of ventilation coefficient on surface concentrations of aerosols

Extensive studies using network station data have shown that the near surface BC concentration over the Indian region is highly sensitive to the boundary layer dynamics (e.g., Babu and Moorthy 2002; Nair *et al.* 2007; Beegum *et al.* 2009; Dunka *et al.* 2010). PBL height and mean wind speed within the PBL play a significant role in the dilution of pollutants within the atmospheric boundary layer. A deeper boundary layer would allow mixing of aerosols to higher heights and hence reduce surface concentrations. Wind speed governs the advection and mixing. Ventilation coefficient ( $VC$ ), a product of PBL height ( $Z_i$ ) and mean (transport) wind speed ( $U_T$ ) within the boundary layer combines these effects into a single parameter.

$$VC = Z_i \times U_T. \quad (1)$$

We estimated the correlation coefficients between VC and surface BC, for the model and the available observations (table 7). [For the model, we have taken the surface winds (and not the mean winds within boundary layer) for calculating the ventilation coefficients. The wind and PBL height values were averaged for grid points surrounding an observation station. In order to find correlation between VC and BC in observations, we have resorted to MERRA reanalysis dataset for wind speeds and PBL height values and then computed the VC values. We compared PBL heights from MERRA with those estimated from radiosonde data and found good comparison between the two and hence used that in our study.] It is seen that (table 7), with a few exceptions, VC has a negative correlation with BC concentration at the surface. Both higher wind speeds and deeper boundary layer help in the dilution of pollutants and hence

such a correlation is expected. So, higher the VC, lesser is the BC surface concentration. It is to be noted that the surface concentrations of BC in model simulations are to some extent driven by meteorology (in addition to the chemistry), with constant emissions, but in reality, emissions will have a diurnal cycle, which will also contribute to the surface concentrations of pollutants. This is reflected in lower correlation between VC and BC in observations than in model. It can also be seen from the table that, model simulated ventilation coefficients are reasonably replicating the variation in VC that is seen in MERRA dataset (indicated by satisfactory correlation between model and MERRA VC). The scatter plots between VC and BC for the months of May and October 2011, for different stations, from model data and observations are shown in figure 11. Model data shows a similar relation between VC and BC as that of observations. The scatter plots are drawn for hourly values of BC and VC for model simulations and observed BC and MERRA VC.

#### 4.3.2 Comparison of ventilation coefficients: Model versus MERRA

In view of the significance of ventilation coefficients on aerosol concentration seen above and also elsewhere (e.g., Nair *et al.* 2007), we have compared the time series of VCs as given by the model and MERRA for two stations, viz., for Bangalore (figures 12a and 13a) and Chennai (figure 13b and c), for May and October 2011. While the model captures the diurnal variation of VC, it fails to simulate the day-to-day variation of daily maximum value of VC as seen in MERRA data. Model simulated values of ventilation coefficient are generally higher (by a factor between 2 and 3) than the corresponding MERRA values (figures 12 and 13). The large overestimation of ventilation coefficient by model could be a probable cause of underestimation of BC concentrations in the PBL.

Table 7. Correlation coefficient ( $CC$ ) between ventilation coefficient and BC mass concentrations for model simulations and MERRA data, for various stations over India. Significance levels of  $CC$ : Trivandrum, Model VC-MERRA VC in Oct, 97%, Rest of them – more than 99%.

Station	Month	CC:VC and BC (model)	CC:VC (MERRA) and BC (Obs)	CC:model VC and MERRA VC
Bangalore	{ May	-0.5406	-0.3547	0.3754
	{ October	-0.5065	-0.3903	0.2209
Chennai	{ May	-0.2143	-0.2180	0.3073
	{ October	-0.4200	-0.3649	0.4395
Trivandrum	{ May	-0.3432	-0.3474	0.3879
	{ October	-0.4561	0.1673	0.1386

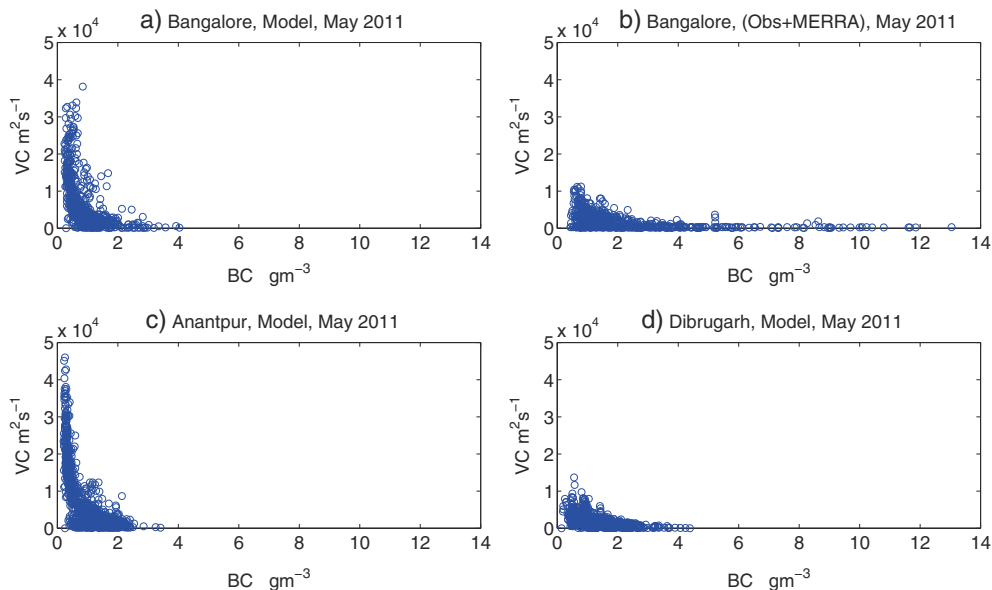


Figure 11. Scatter plots between ventilation coefficients and surface BC mass concentrations from (a) Model simulations over Bangalore, for May 2011, (b) MERRA (VC) and observational BC over Bangalore, for May 2011, (c) Model simulations over Anantpur, for May 2011 and (d) Model simulations over Dibrugarh, for May 2011.

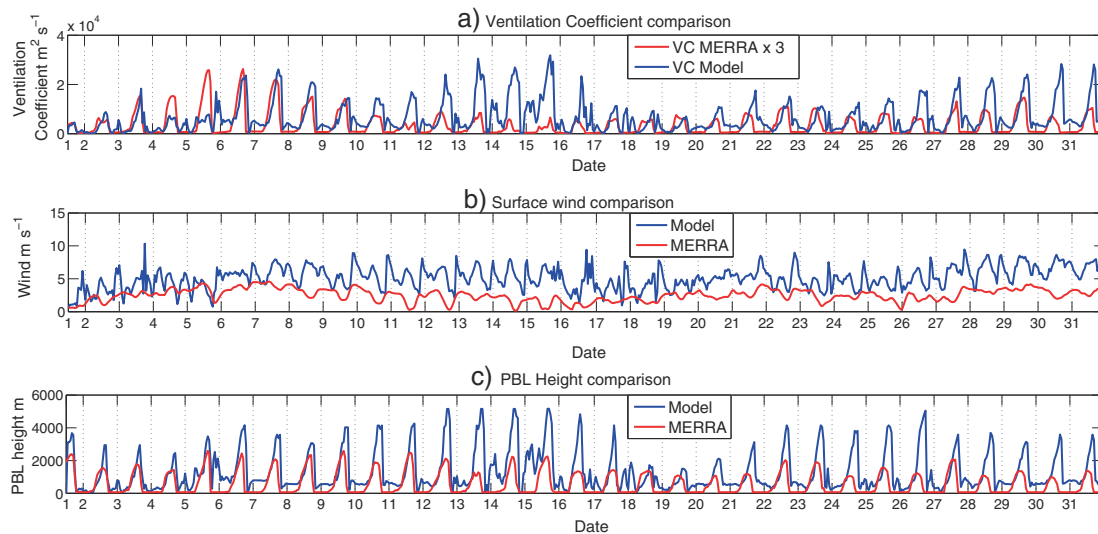


Figure 12. Time-series of meteorological variables over Bangalore, from model simulations and MERRA, for May 2011. (a) Ventilation coefficient, (b) surface wind and (c) PBL height.

With a view of delineating the probable roles of PBL height and horizontal wind leading to the overestimation of VC, we examined the model generated winds and PBL height with the 2-m wind and PBL height from MERRA over Bangalore in figure 12. It is seen that despite the similarity in the variations, the model simulated values of surface wind speed and PBL height are much higher as compared to corresponding MERRA values. As VC is the product of these two, the overestimation gets magnified. Thus the model's capability of simulating the ventilation coefficients needs to be

improved, if the model has to agree better with the BC observations.

Similar to surface BC concentrations, it could be argued that, surface concentrations of dust and sea-salt aerosols are largely driven by atmospheric state variables like  $Z_i$ ,  $U_T$  and rainfall. We examined the time series of surface dust concentration, wind-speed, and PBLH (figure 14a) over a location near Thar desert (northwestern India). It can be seen that surface dust concentration is very strongly related to wind-speeds and PBL height. So, simulations of wind and PBLH can have an



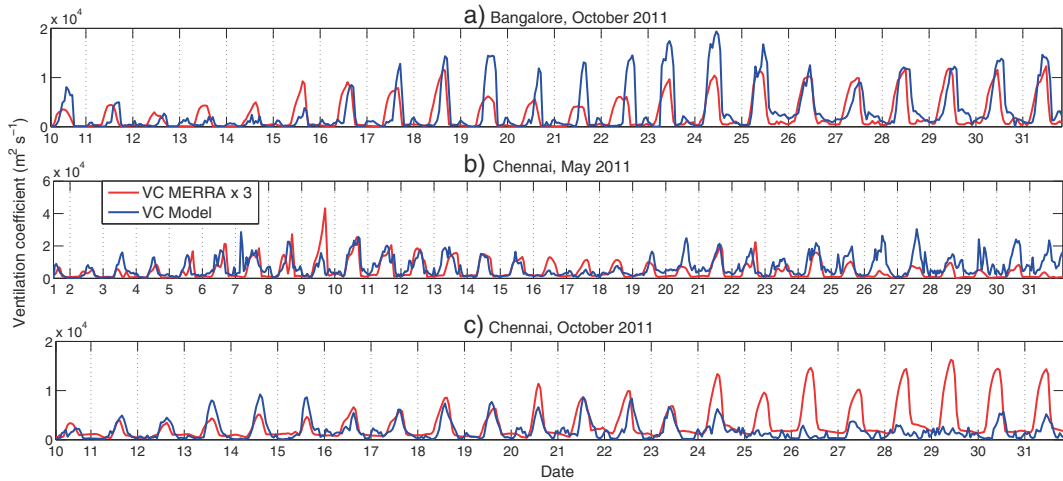


Figure 13. Time series of ventilation coefficient from model simulations and MERRA data over (a) Bangalore, for (b) October 2011 and over Chennai for (b) May 2011 and (c) October 2011.

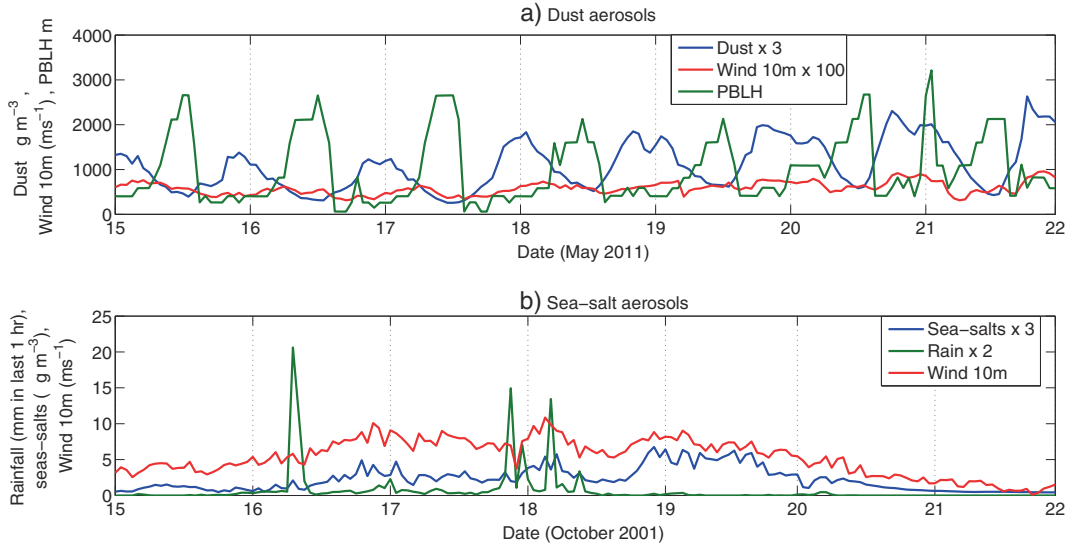


Figure 14. (a) Time-series of surface dust concentration, surface wind magnitudes and PBL height over a location near Thar desert, from WRF-Chem simulations. (b) Time-series of surface sea-salt aerosol concentration, surface wind magnitudes and rainfall over a location within Bay of Bengal, from WRF-Chem simulations.

effect on simulations of dust at the surface. Wind speed influences dust concentration in two ways, viz., surface winds lift the dust into the air and the winds above surface advect the dust from one region to another; while PBL height controls the surface dust concentration by limiting the height over which mixing occurs in the vertical. Similarly, we examined the effects of atmospheric state variables like rainfall and wind speed on the concentrations of sea-salt aerosol. For that we plotted the corresponding time series (figure 14b), it can be seen that winds along with rainfall have a significant impact on sea-salt concentrations at the surface level. Sea-salt is highly hygroscopic and hence scavenging action of rainfall is very

effective in removing sea-salt. Thus, dust, BC, and sea-salt aerosol concentration at the surface are closely associated with meteorological conditions and incorrect simulations meteorology could affect simulations of those aerosol species as well. In addition to the meteorological conditions, the underestimation of aerosol mass concentration could also be related to the use of improper emission inventories in the model simulations. Spatial distribution of AOD (figure 7) gives an impression of an underestimated emission scenario, as the column integrated optical properties of aerosols show lesser values as compared to MODIS. So, an improvement in the overall emission scenario could also help in improving the model's performance in aerosols

simulations. These results are consistent with the results of a few recent studies, such as those by Nair *et al.* (2012) and Moorthy *et al.* (2013a). However, our study differs from these studies in many ways. We have analysed the spatial pattern of TOMS aerosol index over Indian region for the period of 8 years (1996–2003), to decide the months for our model simulations. Moreover, our simulations have considered periods different from the earlier studies, there by examining a temporally and spatially different scenario. While Nair *et al.* (2012) used RegCM and Moorthy *et al.* (2013a) used GOCART and CHIMERE models, we have used WRF-Chem, which is entirely different from the models used in the previous studies. We have a different domain for our simulations in comparison with those two studies. Horizontal resolution of our simulations is 12 km which is significantly finer in comparison with Nair *et al.* (2012) (50 km) and Moorthy *et al.* (2013a) (for GOCART:  $1.25^\circ$  long.  $\times$   $1^\circ$  lat. and for CHIMERE: 100–200 km). WRF-Chem has different sets of physics and chemistry schemes in comparison with that for the models used in Nair *et al.* (2012) and Moorthy *et al.* (2013a). Also, these models use different emission inventories. BC emissions in Nair *et al.* (2012) have been taken from Junker and Liousse (2008), and that in Moorthy *et al.* (2013a) are from an inventory based on Lu *et al.* (2011), while we have used BC emissions from the GOCART database (Chin *et al.* 2002, 2009). We have used an online chemistry transport model in our simulations. Though Nair *et al.* (2012) have used an online-chemistry transport model, the models used in Moorthy *et al.* (2013a) are offline-chemistry transport models. Also, in RegCM4 used in Nair *et al.* (2012), both the direct and indirect effects of aerosols are modelled. The indirect effects are taken into account by assuming dependence of the effective cloud droplet radius on the aerosol mass concentration (Pal *et al.* 2007). While in our WRF-Chem simulations, indirect effects are not modelled as the cloud microphysics scheme employed here is not directly influenced by aerosols. In spite of the mentioned differences in formulation of these three models (i.e., RegCM4 used in Nair *et al.* (2012), GOCART in Moorthy *et al.* (2013a) and WRF-Chem used in this work), we can still observe some robust features in the results from the model simulations. RegCM4 and WRF-Chem show underestimation in AOD, while all the three models (RegCM4, GOCART and WRF-Chem) underestimate near-surface BC values. Performance of the models in simulating aerosol concentrations appears to be affected by formulation of boundary layer parameterization and anthropogenic emissions. So these issues seem to be ubiquitous across the models. All these lead to the inference that,

there is a need to improve boundary layer parameterization and emissions inventory in most of the chemistry transport models while they are used over the (tropical) Indian region.

## 5. Conclusions

In view of the importance in improving the accuracy of aerosol simulations by models, and the absence of a quantitative validation of models over the Indian region, we have examined the capability of the online WRF-Chem model in simulating the aerosol concentrations (both in the vertical column and also within the PBL) and evaluated the model's performance with data from ground-based network observatories, aircraft observations, and MERRA database.

The spatial pattern of winds simulated by WRF-Chem were realistic; however, the magnitudes were generally overestimated. Model simulated spatial pattern of monthly mean rainfall (over the Indian landmass) was in good agreement with that from TRMM, but the model failed to simulate the rainfall time-series, at specific stations, for pre-monsoon and post-monsoon months of 2011. The atmospheric boundary layer heights, which govern the dispersion of pollutants in vertical, were almost 1.5 to 2 times larger in model simulations as compared to that of MERRA.

Model simulated spatial pattern of aerosol optical depth at 550 nm was in good agreement with that from MODIS, but on an average the model AODs were half of the corresponding MODIS values for both the months. This possibly points towards an underestimated emission scenario in model simulations. There is a need to update the emission scenario, to match the current emissions. Model's performance in simulating black carbon (BC) concentration was also examined. It systematically underestimated surface concentrations of black carbon (BC) as compared to the observations made at the ARFINET stations (Bangalore, Chennai, Trivandrum, Hyderabad, Ananthpur, Ranchi, Varanasi, Dibrugarh, and Delhi). Though the model captured the variations, it could not simulate the actual magnitudes. The model did capture the overall pattern of the BC vertical profile over the aircraft observation locations (Port Blair, Bhubaneswar, Hyderabad, and Visakhapatnam), but underestimated BC concentrations vertically. Overall, model underestimated the aerosol scenario over the Indian region. Model's inability in simulating aerosol concentration appeared to be coupled with the emissions scenario (GOCART database) used in the simulations, increased scavenging of particles due to incorrect simulations of rainfall

by the model and the limitations of model in simulating other vital meteorological parameters (PBL height and wind speed). A further analysis of the results of model simulations and reanalysis data showed that, the ventilation coefficient (VC) which is a combination of wind speed within the atmospheric boundary layer and the height of the atmospheric boundary layer, has a high negative correlation with the surface BC concentrations, in most of the cases, in model simulations and in observations. The model systematically overestimated VC, where the peak VC values from the model simulations could be as high as 4 times the values from MERRA, for the same location, for both the months. The overestimates caused lower BC values at the surface. Similar to BC, a strong relation between dust, sea-salt aerosols, and atmospheric state variables like wind speed, rainfall, and atmospheric boundary layer height was also found. So incorrect simulations of meteorological parameters would have also affected simulations of these aerosol species. Hence, improvements in simulation of meteorology within WRF-Chem would be very crucial in improving overall aerosol simulations over the Indian region. Additionally, it is important to note that, the emission inventory used for BC, also needs to be modified to represent the current emission scenario. In this study, we compared model simulations of BC with observations from nine different stations; still it is required to have more number of observational sites for the measurement of aerosol characteristics in order to cover the heterogeneity of the aerosol distribution over the Indian region. Model performance in simulating dust and sea-salt aerosols has not been evaluated here due to lack of observational data for those aerosol species. Comparison of WRF-Chem simulations of aerosols and meteorology over the Indian region with any other chemistry transport model simulations could also be done, but it is not a part of the present study. Overall, it is concluded that, the necessary improvements in the simulations of meteorological variables and the emission inventory would be very vital in improving the aerosol simulations of WRF-Chem over the Indian region.

### Acknowledgements

Authors are grateful to the Computational and Information Systems Laboratory (CISL) for the Research Data Archive. Authors wish to thank the British Atmospheric Data Centre, for the TOMS aerosol index data. They also like to thank GVAX project team for their help in setting up the model. Computations were conducted on the DST-FIST supported computational cluster.

### References

- Babu S S and Moorthy K K 2002 Aerosol black carbon over a tropical coastal station in India; *Geophys. Res. Lett.* **29** 13-1-13-4, doi: 10.1029/2002GL015662.
- Beegum S N, Moorthy K K, Babu S S, Satheesh S K, Vinoj V, Badarinath K, Safai P, Devara P, Singh S, Vinod Dumka U and Pant P 2009 Spatial distribution of aerosol black carbon over India during pre-monsoon season; *Atmos. Environ.* **43** 1071-1078, doi: 10.1016/j.atmosenv.2008.11.042.
- Bollasina M A, Ming Y and Ramaswamy V 2011 Anthropogenic aerosols and the weakening of the south Asian summer monsoon; *Science* **334** 502-505, doi: 10.1126/science.1204994.
- Chakraborty A, Satheesh S K, Nanjundiah R S and Srinivasan J 2004 Impact of absorbing aerosols on the simulation of climate over the Indian region in an atmospheric general circulation model; *Ann. Geophys.* **22** 1421-1434, doi: 10.5194/angeo-22-1421-2004.
- Chin M, Ginoux P, Kinne S, Torres O, Holben B N, Duncan B N, Martin R V, Logan J A, Higurashi A and Nakajima T 2002 Tropospheric aerosol optical thickness from the GOCART model and comparisons with satellite and sun photometer measurements; *J. Atmos. Sci.* **59** 461-483, doi: 10.1175/15200469(2002)059<0461:TAOTFT>2.0.CO;2.
- Chin M, Diehl T, Dubovik O, Eck T F, Holben B N, Sinyuk A and Streets D G 2009 Light absorption by pollution, dust, and biomass burning aerosols: A global model study and evaluation with aeronet measurements; *Ann. Geophys.* **27** 3439-3464, <http://www.ann-geophys.net/27/3439/2009/>, doi: 10.5194/angeo-27-3439-2009.
- Chung C E, Ramanathan V and Kiehl J T 2002 Effects of the south Asian absorbing haze on the northeast monsoon and surface-air heat exchange; *J. Climate* **15** 2462-2476, doi: 10.1175/1520-0442(2002)015<2462:EOTSAA>2.0.CO;2.
- Cooke W, Lioussé C, Cachier H and Feichter J 1999 Construction of a  $1^\circ \times 1^\circ$  fossil fuel emission data set for carbonaceous aerosol and implementation and radiative impact in the echam4 model; *J. Geophys. Res.* **104** 22,137-22,162, doi: 10.1029/1999JD900187.
- Dumka U, Moorthy K K, Kumar R, Hegde P, Sagar R, Pant P, Singh N and Babu S S 2010 Characteristics of aerosol black carbon mass concentration over a high altitude location in the central Himalayas from multi-year measurements; *Atmos. Res.* **96** 510-521, doi: 10.1016/j.atmosres.2009.12.010.
- Emmons L K, Walters S, Hess P G, Lamarque J F, Pfister G G, Fillmore D, Granier C, Guenther A, Kinnison D, Laepple T, Orlando J, Tie X, Tyndall G, Wiedinmyer C, Baughcum S L and Kloster S 2010 Description and evaluation of the model for Ozone and related chemical tracers, version 4 (MOZART-4); *Geoscientific Model Development* **3** 43-67, doi: 10.5194/gmd-3-43-2010.
- Freitas S R, Longo K M, Alonso M F, Pirre M, Marecal V, Grell G, Stockler R, Mello R F and Sánchez Gácita M 2011 Prep-chem-src 1.0: A preprocessor of trace gas and aerosol emission fields for regional and global atmospheric chemistry models; *Geoscientific Model Development* **4** 419-433, <http://www.geosci-model-dev.net/4/419/2011/>, doi: 10.5194/gmd-4-419-2011.
- Ganguly D, Rasch P J, Wang H and Yoon J H 2012 Climate response of the south Asian monsoon system to anthropogenic aerosols; *J. Geophys. Res.: Atmospheres* **117**, doi: 10.1029/2012JD017508.

- Gautam R, Hsu N, Lau K and Kafatos M 2009 Aerosol and rainfall variability over the Indian monsoon region: Distributions, trends and coupling; *J. Geophys. Res.: Atmospheres* **27** 3691–3703, doi: 10.5194/angeo-27-3691-2009.
- Ginoux P, Chin M, Tegen I, Prospero J M, Holben B, Dubovik O and Lin S J 2001 Sources and distributions of dust aerosols simulated with the gocart model; *J. Geophys. Res.: Atmospheres* **106** 20,255–20,273, doi: 10.1029/2000JD000053.
- Haywood J and Boucher O 2000 Estimates of the direct and indirect radiative forcing due to tropospheric aerosols: A review; *Rev. Geophys.* **38** 513–543, doi: 10.1029/1999RG000078.
- Haywood J M and Ramaswamy V 1998 Global sensitivity studies of the direct radiative forcing due to anthropogenic sulfate and black carbon aerosols; *J. Geophys. Res.: Atmospheres* **103** 6043–6058, doi: 10.1029/97JD03426.
- Herman J R, Bhartia P K, Torres O, Hsu C, Seftor C and Celarier E 1997 Global distribution of UV-absorbing aerosols from Nimbus 7/TOMS data; *J. Geophys. Res.: Atmospheres* **102** 16,911–16,922, doi: 10.1029/96JD03680.
- Janjić Z I 2002 Nonsingular implementation of the Mellor-Yamada level 2.5 scheme in the NCEP meso model; NCEP Office Note, 437, 61.
- Jethva H, Satheesh S K and Srinivasan J 2007 Evaluation of moderate-resolution imaging spectroradiometer (MODIS) collection 004 (c004) aerosol retrievals at Kanpur, Indo-Gangetic basin; *J. Geophys. Res.: Atmospheres* **112**, doi: 10.1029/2006JD007929.
- Jethva H, Satheesh S, Srinivasan J and Moorthy K 2009 How good is the assumption about visible surface reflectance in MODIS aerosol retrieval over land? A comparison with aircraft measurements over an urban site in India; *Geosci. Remote Sens. IEEE Trans.* **47**, doi: 10.1109/TGRS.2008.2010221.
- Jones A M and Harrison R M 2004 The effects of meteorological factors on atmospheric bioaerosol concentrations: A review; *Sci. Total Environ.* **326** 151–180, doi: 10.1016/j.scitotenv.2003.11.021.
- Junker C and Liousse C 2008 A global emission inventory of carbonaceous aerosol from historic records of fossil fuel and biofuel consumption for the period 1860–1997; *Atmos. Chem. Phys.* **8** 1195–1207, <http://www.atmos-chem-phys.net/8/1195/2008/>, doi: 10.5194/acp-8-1195-2008.
- Kahn R A, Garay M J, Nelson D L, Yau K K, Bull M A, Gaitley B J, Martonchik J V and Levy R C 2007 Satellite-derived aerosol optical depth over dark water from MISR and MODIS: Comparisons with AERONET and implications for climatological studies; *J. Geophys. Res.: Atmospheres* **112**, doi: 10.1029/2006JD008175.
- Kaufman Y J, Tanré D, Boucher O et al. 2002 A satellite view of aerosols in the climate system; *Nature* **419** 215–223, doi: 10.1038/nature01091.
- Kiran R V, Rajeevan M, Vijaya Bhaskara Rao S and Prabhakara Rao N 2009 Analysis of variations of cloud and aerosol properties associated with active and break spells of Indian summer monsoon using MODIS data; *Geophys. Res. Lett.* **36**, doi: 10.1029/2008GL037135.
- Krishnamurti T N, Chakraborty A, Martin A, Lau W K, Kim K M, Sud Y and Walker G 2009 Impact of Arabian Sea pollution on the Bay of Bengal winter monsoon rains; *J. Geophys. Res.: Atmospheres* **114**, doi: 10.1029/2008JD010679.
- Kumar R, Naja M, Pfister G G, Barth M C and Brasseur G P 2011 Simulations over south Asia using the weather research and forecasting model with chemistry (WRF-Chem): Set-up and meteorological evaluation; *Geoscientific Model Development Discussions* **4** 3067–3125, doi: 10.5194/gmdd-4-3067-2011.
- Kumar R, Naja M, Pfister G G, Barth M C, Wiedinmyer C and Brasseur G P 2012 Simulations over south Asia using the weather research and forecasting model with chemistry (WRF-Chem): Chemistry evaluation and initial results; *Geoscientific Model Development* **5** 619–648, doi: 10.5194/gmd-5-619-2012.
- Lau K, Kim M and Kim K 2006 Asian summer monsoon anomalies induced by aerosol direct forcing: The role of the Tibetan plateau; *Clim. Dyn.* **26** 855–864, doi: 10.1007/s00382-006-0114-z.
- Levy R C, Remer L A, Kleidman R G, Mattoo S, Ichoku C, Kahn R and Eck T F 2010 Global evaluation of the collection 5 MODIS dark-target aerosol products over land; *Atmospheric Chemistry and Physics Discussions* **10** 14,815–14,873, doi: 10.5194/acpd-1014815-2010.
- Lohmann U and Feichter J 2005 Global indirect aerosol effects: A review; *Atmos. Chem. Phys.* **5** 715–737, doi: 10.5194/acp-5-715-2005.
- Lohmann U and Lesins G 2002 Stronger constraints on the anthropogenic indirect aerosol effect; *Science* **298** 1012–1015, doi: 10.1126/science.1075405.
- Lu Z, Zhang Q and Streets D G 2011 Sulfur dioxide and primary carbonaceous aerosol emissions in china and india, 1996–2010; *Atmos. Chem. Phys.* **11** 9839–9864, <http://www.atmos-chem-phys.net/11/9839/2011/>, doi: 10.5194/acp-119839-2011.
- Meehl G A, Arblaster J M and Collins W D 2008 Effects of black carbon aerosols on the Indian monsoon; *J. Climate* **21** 2869–2882, doi: 10.1175/2007JCLI1777.1.
- Menon S, Hansen J, Nazarenko L and Luo Y 2002 Climate effects of black carbon aerosols in China and India; *Science* **297** 2250–2253, doi: 10.1126/science.1075159.
- Mlawer E J, Taubman S J, Brown P D, Iacono M J and Clough S A 1997 Radiative transfer for inhomogeneous atmospheres: RRTM, a validated correlated-k model for the longwave; *J. Geophys. Res.: Atmospheres* **102** 16,663–16,682, doi: 10.1029/97JD00237.
- Moorthy K K and Satheesh S 2011 Black carbon aerosols over India; *UNEPs Black Carbon e-Bulletin* **3** 1–3.
- Moorthy K K, Babu S S, Satheesh S K, Srinivasan J and Dutt C B S 2007 Dust absorption over the great Indian desert inferred using ground-based and satellite remote sensing; *J. Geophys. Res.: Atmospheres* **112**, doi: 10.1029/2006JD007690.
- Moorthy K, Satheesh S, Babu S and Dutt C 2008 Integrated Campaign for Aerosols, gases and Radiation Budget (ICARB): An overview; *J. Earth Syst. Sci.* **117** 243–262, doi: 10.1007/s12040-008-0029-7.
- Moorthy K K, Nair V S, Babu S S and Satheesh S K 2009 Spatial and vertical heterogeneities in aerosol properties over oceanic regions around India: Implications for radiative forcing; *Quart. J. Roy. Meteor. Soc.* **135** 2131–2145, doi: 10.1002/qj.525.
- Moorthy K K, Beegum S N, Babu S S, Smirnov A, John S R, Kumar K R, Narasimhulu K, Dutt C B S and Nair V S 2010 Optical and physical characteristics of Bay of Bengal aerosols during W-ICARB: Spatial and vertical heterogeneities in the marine atmospheric boundary layer and in the vertical column; *J. Geophys. Res.: Atmospheres* **115**, doi: 10.1029/2010JD014094.
- Moorthy K K, Beegum S N, Srivastava N, Satheesh S, Chin M, Blond N, Babu S S and Singh S 2013a Performance evaluation of chemistry transport models over India; *Atmos. Environ.* **71** 210–225, doi: 10.1016/j.atmosenv.2013.01.056.

- Moorthy K K, Babu S S, Manoj M R and Satheesh S K 2013b Buildup of aerosols over the Indian region; *Geophys. Res. Lett.*, doi: 10.1002/grl.50165.
- Myhre G 2009 Consistency between satellite-derived and modeled estimates of the direct aerosol effect; *Science* **325** 187–190, doi: 10.1126/science.1174461.
- Nair V S, Moorthy K K, Alappattu D P, Kunhikrishnan P K, George S, Nair P R, Babu S S, Abish B, Satheesh S K, Tripathi S N, Niranjan K, Madhavan B L, Srikant V, Dutt C B S, Badarinath K V S and Reddy R R 2007 Wintertime aerosol characteristics over the Indo-Gangetic Plain (IGP): Impacts of local boundary layer processes and long-range transport; *J. Geophys. Res.: Atmospheres* **112**, doi: 10.1029/2006JD008099.
- Nair V S, Solmon F, Giorgi F, Mariotti L, Babu S S and Moorthy K K 2012 Simulation of south Asian aerosols for regional climate studies; *J. Geophys. Res.: Atmospheres* **117**, doi: 10.1029/2011JD016711.
- Olivier J G J, Bouwman A, Berdowski J, Veldt C, Bloos J, Visschedijk A, Zandveld P and Haverla J *et al.* 1996 Description of EDGAR version 2.0: A set of global emission inventories of greenhouse gases and ozone-depleting substances for all anthropogenic and most natural sources on a per country basis and on  $1^\circ \times 1^\circ$  grid, Bilthoven, Netherlands, Rijksinstituut voor Volksgezondheid en Milieu RIVM.
- Pal J S, Giorgi F, Bi X, Elguindi N, Solmon F, Rauscher S A, Gao X, Francisco R, Zakey A, Winter J, Ashfaq M, Syed F S, Sloan L C, Bell J L, Diffenbaugh N S, Karmacharya J, Konar A, Martinez D, da Rocha R P and Steinerh A L 2007 Regional climate modeling for the developing world: The ICTP RegCM3 and RegCNET; *Bull. Am. Meteorol. Soc.* **88** 1395–1409, doi: 10.1175/BAMS-889-1395.
- Ramanathan V, Crutzen P J, Lelieveld J, Mitra A P, Althausen D, Anderson J, Andreae M O, Cantrell W, Cass G R, Chung C E, Clarke A D, Coakley J A, Collins W D, Conant W C, Dulac F, Heintzenberg J, Heymsfield A J, Holben B, Howell S, Hudson J, Jayaraman A, Kiehl J T, Krishnamurti T N, Lubin D, McFarquhar G, Novakov T, Ogren J A, Podgorny I A, Prather K, Priestley K, Prospero J M, Quinn P K, Rajeev K, Rasch P, Rupert S, Sadourny R, Satheesh S K, Shaw G E, Sheridan P and Valero F P J 2001 Indian Ocean experiment: An integrated analysis of the climate forcing and effects of the great Indo-Asian haze; *J. Geophys. Res.: Atmospheres* **106** 28,371–28,398, doi: 10.1029/2001JD900133.
- Ramanathan V, Chung C, Kim D, Bettge T, Buja L, Kiehl J, Washington W, Fu Q, Sikka D and Wild M 2005 Atmospheric brown clouds: Impacts on south Asian climate and hydrological cycle; *Proc. National Academy of Sciences of the United States of America* **102** 5326–5333, doi: 10.1073/pnas.0500656102.
- Remer L A, Kaufman Y, Tanré D, Mattoo S, Chu D, Martins J, Li R R, Ichoku C, Levy R and Kleidman R *et al.* 2005 The MODIS aerosol algorithm, products, and validation; *J. Atmos. Sci.* **62** 947–973, doi: 10.1175/JAS3385.1.
- Rienecker M M, Suarez M J, Gelaro R, Todling R, Bacmeister J, Liu E, Bosilovich M G, Schubert S D, Takacs L and Kim G K *et al.* 2011 MERRA: NASA's modern-era retrospective analysis for research and applications; *J. Climate* **24** 3624–3648, doi: 10.1175/JCLI-D-11-00015.1.
- Sajani S, Krishnamoorthy K, Rajendran K and Nanjundiah R S 2012 Monsoon sensitivity to aerosol direct radiative forcing in the Community Atmosphere Model; *J. Earth Syst. Sci.* **121** 867–889, doi: 10.1007/s12040-012-0198-2.
- Sánchez-Ccoyllo O and de Fátima Andrade M 2002 The influence of meteorological conditions on the behaviour of pollutants concentrations in São Paulo, Brazil; *Environ. Pollut.* **116** 257–263, doi: 10.1016/S0269-7491(01)00129-4.
- Satheesh S and Moorthy K K 2005 Radiative effects of natural aerosols: A review; *Atmos. Environ.* **39** 2089–2110, doi: 10.1016/j.atmosenv.2004.12.029.
- Schultz M, Backman L, Balkanski Y, Bjoerndalsaeter S, Brand R, Burrows J, Dalsoeren S, de Vasconcelos M, Grodtmann B and Hauglustaine D *et al.* 2007 REanalysis of the TROpospheric chemical composition over the past 40 years (RETRO) – a long-term global modeling study of tropospheric chemistry, Final Report, Published as report no. 48/2007 in the series Reports on Earth System Science of the Max Planck Institute for Meteorology, Hamburg, ISSN 1614–1199.
- Skamarock W, Klemp J, Dudhia J, Gill D, Barker D, Duda M, Huang X, Wang W and Powers J 2008 A description of the advanced research WRF version 3. NCAR technical note NCAR/TN-475+STR, doi: 10.5065/D68S4MVH.
- Smirnova T G, Brown J M and Benjamin S G 1997 Performance of different soil model configurations in simulating ground surface temperature and surface fluxes; *Mon. Wea. Rev.* **125** 1870–1884, doi: 10.1175/1520-0493(1997)125<1870:PODSMC>2.0.CO;2.
- Smirnova T G, Brown J M, Benjamin S G and Kim D 2000 Parameterization of cold-season processes in the maps land-surface scheme; *J. Geophys. Res.: Atmospheres* **105** 4077–4086, doi: 10.1029/1999JD901047.
- Sreekanth V, Krishna Moorthy K, Satheesh S, Suresh Babu S, Nair V S and Niranjan K 2011 Airborne measurements of aerosol scattering properties above the MABL over Bay of Bengal during W-ICARB-characteristics and spatial gradients; In: *Annales Geophysicae*, Copernicus Group, pp. 895–908, doi: 10.5194/angeo-29-895-2011.
- Takemura T, Nozawa T, Emori S, Nakajima T Y and Nakajima T 2005 Simulation of climate response to aerosol direct and indirect effects with aerosol transport-radiation model; *J. Geophys. Res.: Atmospheres* **110**, doi: 10.1029/2004JD005029.
- Tao W K, Chen J P, Li Z, Wang C and Zhang C 2012 Impact of aerosols on convective clouds and precipitation; *Rev. Geophys.* **50**, doi: 10.1029/2011RG000369.
- Thompson G, Rasmussen R M and Manning K 2004 Explicit forecasts of winter precipitation using an improved bulk microphysics scheme. Part 1: Description and sensitivity analysis; *Mon. Wea. Rev.* **132** 519–542, doi: 10.1175/1520-0493(2004)132<0519:EFOWPU>2.0.CO;2.
- Twomey S 1977 The influence of pollution on the short-wave albedo of clouds; *J. Atmos. Sci.* **34** 1149–1152, doi: 10.1175/1520-0469(1977)034<1149:TIOPOT>2.0.CO;2.
- Wang C, Kim D, Ekman A M L, Barth M C and Rasch P J 2009 Impact of anthropogenic aerosols on Indian summer monsoon; *Geophys. Res. Lett.* **36**, doi: 10.1029/2009GL040114.
- Wehner B and Wiedensohler A 2002 Long term measurements of submicrometer urban aerosols: Statistical analysis for correlations with meteorological conditions and trace gases; *Atmospheric Chemistry and Physics Discussions* **2** 1699–1733, doi: 10.5194/acpd-2-16992002.
- Wild O, Zhu X and Prather M 2000 Fast-j: Accurate simulation of in- and below-cloud photolysis in tropospheric chemical models; *J. Atmos. Chem.* **37** 245–282, doi: 10.1023/A:1006415919030.
- Yu H, Kaufman Y J, Chin M, Feingold G, Remer L A, Anderson T L, Balkanski Y, Bellouin N, Boucher O, Christopher S, DeCola P, Kahn R, Koch D, Loeb N, Reddy M S, Schulz M, Takemura T and Zhou M 2006 A review of measurement-based assessments of the aerosol direct radiative effect and forcing; *Atmos. Chem. Phys.* **6** 613–666, doi: 10.5194/acp-6-613-2006.

- Zhang G J and McFarlane N A 1995 Sensitivity of climate simulations to the parameterization of cumulus convection in the Canadian climate centre general circulation model; *Atmosphere-Ocean* **33** 407–446, doi: 10.1080/07055900.1995.9649539.
- Zhang J, Christopher S A, Remer L A and Kaufman Y J 2005 Shortwave aerosol radiative forcing over cloud-free oceans from TERRA: 2. Seasonal and global distributions; *J. Geophys. Res.: Atmospheres* **110**, doi: 10.1029/2004JD005009.

*MS received 26 August 2014; revised 13 January 2015; accepted 14 January 2015*